Published in final edited form as:

Nat Genet. 2022 September ; 54(9): 1320–1331. doi:10.1038/s41588-022-01104-0.

✉**Correspondence and requests for materials** should be addressed to Joseph D. Buxbaum, Mark J. Daly, Bernie Devlin, Kathryn Roeder, Stephan J. Sanders or Michael E. Talkowski. joseph.buxbaum@mssm.edu; mjdaly@atgu.mgh.harvard.edu; devlinbj@upmc.edu; roeder@andrew.cmu.edu; Stephan.Sanders@ucsf.edu; MTALKOWSKI@mgh.harvard.edu.

*Lists of authors and their affiliations appear at the end of the paper.

Author contributions

M.E.T., S.J.S, K.R., B.D., M.J.D, J.D.B. and S.B.G. designed the study. M.E.T., M.J.D., J.D.B., S.D.R., S.B.G., S.D., C.C., C.R.S., M.B, A.B, B.H.Y.C., M.L.C., E.D, G.B.F., J.J.G., G.E.H., I.H.-P., P.M., D.S.M., M.R.P.-B., A.M.P., A.R., F.T., E.T., G.C., M.C.Y.C., C.F., E.G., A.C.G., E.H.-K., S.L.L., C.L., Y.L., R.N., L.P., M.P-V., I.N.P., R.J.S., M.S., C.I.S.C., S.T., J.Y.T.W., M.H.C.Y., J.S.S., E.H.C. and C.B. contributed samples and generated data. M.E.T., S.J.S., M.J.D., J.D.B., S.D.R., L.S., B.M., C.R.S. and B.C. coordinated project management. M.E.T., S.J.S., K.R., B.D., M.J.D., D.J.C., E.B., A.N.S., M.B., S.K.L., L.G., B.W., L.K., L.W., S.P.H. S.D., R.L.C., H.B., M.P., F.K.S. and J.M.F. developed methodology and performed analysis. M.E.T., S.J.S., K.R., B.D., M.J.D., J.D.B., H.B., M.P., F.K.S. and J.M.F. wrote the paper.

Competing interests

C.M.F. has been a consultant to Desitin and Roche and receives royalties for books on ASD, ADHD, and MDD. S.J.S. has been a consultant for, and receives funding for research from, BioMarin. J.D.B. and M.E.T. consult for BrigeBio Pharma. M.E.T. receives research funding and/or reagents from Illumina Inc., Levo Therapeutics, and Microsoft Inc. All other authors had no competing interests.

Additional information

Supplementary information The online version contains supplementary material available at https://doi.org/10.1038/s41588-022-01104-0.

Peer review information *Nature genetics* thanks Maria Chahrour and Zilong Qiu for their contribution to the peer review of this work.

Reprints and permissions information is available at www.nature.com/reprints.

The Autism Sequencing Consortium (ASC)

Branko Aleksic[50], Mykyta Artomov[1,2,4,47], Mafalda Barbosa[15,18], Elisa Benetti[34,35], Catalina Betancur[19], Monica Biscaldi-Schafer[51], Anders D. Børglum[52,53,54,55], Harrison Brand[1,2,3,7,82], Alfredo Brusco[20,21], Joseph D. Buxbaum[13,14,15,18,45,46], Gabriele Campos[32], Simona Cardaropoli[26], Diana Carli[26], Angel Carracedo[56,57], Marcus C. Y. Chan[22], Andreas G. Chiocchetti[50], Brian H. Y. Chung[22], Brett Collins[13,14,15], Ryan L. Collins[1,2,3,8], Edwin H. Cook[23], Hilary Coon[58,59], Claudia I. S. Costa[32], Michael L. Cuccaro[24], David J. Cutler[44], Mark J. Daly[1,2,4,5,47,48], Silvia De Rubeis[13,14,15,45], Bernie Devlin[11], Ryan N. Doan[60], Enrico Domenici[25], Shan Dong[9], Chiara Fallerini[34,35], Montserrat Fernández-Prieto[56,61], Giovanni Battista Ferrero[26], Christine M. Freitag[50], Jack M. Fu[1,2,3,82], J. Jay Gargus[27], Sherif Gerges[1,2,4,47], Elisa Giorgio[20], Ana Cristina Girardi[32], Stephen Guter[23], Emily Hansen-Kiss[41], Gail E. Herman[28], Irva Hertz-Picciotto[29], David M. Hougaard[51,62], Christina M. Hultman[17], Suma Jacob[23], Miia Kaartinen[63], Lambertus Klei[11], Alexander Kolevzon[13,14,64], Itaru Kushima[52,65], So Lun Lee[22], Terho Lehtimäki[66], Lindsay Liang[9], Carla Lintas[42], Alicia Ljungdahl[9], Caterina Lo Rizzo[35,36], Yunin Ludena[29], Patricia Maciel[30], Behrang Mahjani[13,14,17], Nell Maltman[23], Marianna Manara[35,36], Dara S. Manoach[31], Gal Meiri[67,68], Idan Menashe[69,70], Judith Miller[71,72], Nancy Minshew[11], Matthew Mosconi[73], Rachel Nguyen[27], Norio Ozaki[52,74], Aarno Palotie[2,5,48,75], Mara Parellada[76], Maria Rita Passos-Bueno[32], Lisa Pavinato[20], Minshi Peng[6,82], Margaret Pericak-Vance[24], Antonio M. Persico[33], Isaac N. Pessah[29,43], Kaija Puura[63], Abraham Reichenberg[13,14,15,77], Alessandra Renieri[34,35,36], Kathryn Roeder[6,49], Stephan J. Sanders[9], Sven Sandin[13,14,17], F. Kyle Satterstrom[2,4,5,82], Stephen W. Scherer[78,79], Sabine Schlitt[50], Rebecca J. Schmidt[29], Lauren Schmitt[23], Katja Schneider-Momm[50], Paige M. Siper[13,14,15], Laura Sloofman[13,14,15], Moyra Smith[27], Christine R. Stevens[2,4,5], Pål Suren[80], James S. Sutcliffe[37,38], John A. Sweeney[81], Michael E. Talkowski[1,2,3,4,8], Flora Tassone[29,39], Karoline Teufel[50], Elisabetta Trabetti[40], Slavica Trajkova[20], Maria del Pilar Trelles[13,14], Brie Wamsley[10], Jaqueline Y. T. Wang[32], Lauren A. Weiss[9], Mullin H. C. Yu[22] and Ryan Yuen[78]

[50]Department of Psychiatry, Graduate School of Medicine, Nagoya University, Nagoya, Japan. [51]Department of Child and Adolescent Psychiatry, Psychosomatics and Psychotherapy, Goethe University Frankfurt, Frankfurt, Germany. [52]The Lundbeck Foundation Initiative for Integrative Psychiatric Research, iPSYCH, Aarhus, Denmark. [53]Department of Biomedicine—Human Genetics, Aarhus University, Aarhus, Denmark. [54]Center for Genomics and Personalized Medicine, Aarhus, Denmark. [55]Bioinformatics Research Centre, Aarhus University, Aarhus, Denmark. [56]Grupo de Medicina Xenómica, Centro de Investigación en Red de Enfermedades Raras (CIBERER), CIMUS, Universidade de Santiago de Compostela, Santiago de Compostela, Spain. [57]Fundación Pública Galega de Medicina Xenómica, Servicio Galego de Saúde (SERGAS), Santiago de Compostela, Spain. [58]Department of Internal Medicine, University of Utah, Salt Lake City, UT, USA. [59]Department of Psychiatry, Huntsman Mental Health Institute, University of Utah, Salt Lake City, UT, USA. [60]Division of Genetics and Genomics, Boston Children's Hospital, Boston, MA, USA. [61]Neurogenetics group, Instituto de Investigación Sanitaria de Santiago (IDIS-SERGAS), Santiago de Compostela, Spain. [62]Center for Neonatal Screening, Department for Congenital Disorders, Statens Serum Institut, Copenhagen, Denmark. [63]Department of Child Psychiatry, Tampere University and Tampere University Hospital, Tampere, Finland. [64]Department of Pediatrics, Icahn School of Medicine at Mount Sinai, New York, NY, USA. [65]Medical Genomics Center, Nagoya University Hospital, Nagoya, Japan. [66]Department of Clinical Chemistry, Fimlab Laboratories and Finnish Cardiovascular Research Center-Tampere, Faculty of Medicine and Health Technology, Tampere University, Tampere, Finland. [67]The Azrieli National Center for Autism and Neurodevelopment Research, Ben-Gurion University of the Negev, Beer-Sheva, Israel. [68]Pre-School Psychiatry Unit, Soroka University Medical Center, Beer Sheva, Israel. [69]Department of Public Health, Ben-Gurion University of the Negev, Beer-Sheva, Israel. [70]National Autism Research Center of Israel, Ben-Gurion University of the Negev, Beer-Sheva, Israel. [71]Children's

Rare coding variation provides insight into the genetic architecture and phenotypic context of autism

A full list of authors and affiliations appears at the end of the article.

Abstract

Some individuals with autism spectrum disorder (ASD) carry functional mutations rarely observed in the general population. We explored the genes disrupted by these variants from joint analysis of protein-truncating variants (PTVs), missense variants and copy number variants (CNVs) in a cohort of 63,237 individuals. We discovered 72 genes associated with ASD at false discovery rate (FDR) ≤ 0.001 (185 at FDR ≤ 0.05). De novo PTVs, damaging missense variants and CNVs represented 57.5%, 21.1% and 8.44% of association evidence, while CNVs conferred greatest relative risk. Meta-analysis with cohorts ascertained for developmental delay (DD) (n = 91,605) yielded 373 genes associated with ASD/DD at FDR ≤ 0.001 (664 at FDR ≤ 0.05), some of which differed in relative frequency of mutation between ASD and DD cohorts. The DD-associated genes were enriched in transcriptomes of progenitor and immature neuronal cells, whereas genes showing stronger evidence in ASD were more enriched in maturing neurons and overlapped with schizophrenia-associated genes, emphasizing that these neuropsychiatric disorders may share common pathways to risk.

ASD affects approximately 2.3% of children in the United States[1]. ASD is highly heritable[2], with most genetic risk stemming from common variants, each of small effect, acting additively across the genome[3]. However, in at least 10% of ASD cases, rare and de novo variants confer substantial risk, and exome sequencing has enabled rare coding variant studies across ASD and many related developmental and neuropsychiatric disorders[4–7]. These studies have focused on single nucleotide variants (SNVs) and insertions/deletions (indels) that arise de novo, although modest overtransmission to ASD probands has been observed for some classes of rare inherited variants[4,8,9]. The relative contribution of de novo PTVs to risk varies significantly by ascertainment strategy: burden is greatest in cohorts ascertained for individuals with DD, intellectual disability (ID) or multisystem congenital anomalies; moderate in individuals with ASD or isolated developmental anomalies and

Hospital of Philadelphia, Philadelphia, PA, USA. [72]Department of Psychiatry, University of Utah, Salt Lake City, UT, USA. [73]Life Span Institute and Kansas Center for Autism Research and Training, University of Kansas, Lawrence, KS, USA. [74]Institute for Glycocore Research (iGCORE), Nagoya University, Nagoya, Japan. [75]Psychiatric & Neurodevelopmental Genetics Unit, Department of Psychiatry, Massachusetts General Hospital, Boston, MA, USA. [76]Department of Child and Adolescent Psychiatry, Hospital General Universitario Gregorio Marañón, IiSGM, CIBERSAM, School of Medicine Complutense University, Madrid, Spain. [77]Department of Environmental Medicine and Public Health, Icahn School of Medicine at Mount Sinai, New York, NY, USA. [78]Program in Genetics and Genome Biology, The Centre for Applied Genomics, The Hospital for Sick Children, Toronto, Ontario, Canada. [79]Department of Molecular Genetics and McLaughlin Centre, University of Toronto, Toronto, Ontario, Canada. [80]Norwegian Institute of Public Health, Oslo, Norway. [81]Department of Psychiatry, University of Cincinnati, Cincinnati, OH, USA.

Broad Institute Center for Common Disease Genomics (Broad-CCDG)
Caroline Cusick[4], Christine R. Stevens[2,4,5], Stacey B. Gabriel[16], Mark J. Daly[1,2,4,5,47,48] and Michael E. Talkowski[1,2,3,4,8]
iPSYCH-BROAD Consortium
F. Kyle Satterstrom[2,4,5,82], Christine R. Stevens[2,4,5] and Mark J. Daly[1,2,4,5,47,48]

lowest in schizophrenia and other neuropsychiatric disorders[4,5,7,10,11]. Hundreds of risk genes have been discovered across these disorders, with associations driven largely by phenotypic severity and cohort size[12,13].

Early microarray studies established that individuals with ASD also harbor an excess of very large CNVs[14–19]. These studies identified many recurrent genomic disorder (GD) loci, or recurrent CNVs associated with syndromic features, most of which arose due to mispairing of long homologous segments—a mechanism known as nonallelic homologous recombination (NAHR)[14,16,20,21]. Due to their high mutation rate, NAHR-mediated GDs are among the best characterized genetic risk factors across all neurodevelopmental disorders (NDDs)[6,16,21,22]. Beyond these large segments, defining the contribution of small CNVs localized to individual genes in ASD across large cohorts has been a technical challenge. With advancing technologies, structural variant (SV) discovery is now tractable from whole-genome sequencing (WGS) and has been applied to population resources[23–25], but only to relatively small ASD cohorts[26–30]. These studies, as well as long-read WGS on a small number of individuals[31,32], have shown the mutational diversity of SVs that exist in all genomes, greater than 99% of which were not detectable by previous microarray studies[32,33]. We demonstrate here that refined models of exome-based CNV discovery can capture small, rare, coding CNVs with a sensitivity and specificity that is comparable to indel discovery and amenable to large-scale association studies. We reasoned that joint analyses of rare coding SNVs, indels and CNVs at the resolution of individual genes and exons in large cohorts would provide a more complete picture of allelic diversity and mutational mechanisms that impact specific genes contributing to ASD.

Discovery of risk genes can also be enhanced through the integration of functional effects of rare variation and metrics to quantify negative selection[4]. One such measure is the ‘loss-of-function observed/expected upper bound fraction’ (LOEUF) score[34], which is a continuous measure of selective pressure against PTVs in each gene. Similarly, the ‘missense badness, PolyPhen-2, and constraint’ (MPC) score[35] is a measure of the estimated deleteriousness of missense variation. In this study, we use a Bayesian statistical framework, the transmission and de novo association (TADA) model[36], to incorporate these functional annotations into joint analyses of coding SNVs, indels and CNVs across the largest exome-sequenced ASD and DD cohorts at the time of analysis, comprising 63,237 individuals from ASD cohorts (20,627 ASD-affected individuals) and 91,605 samples from DD cohorts (31,058 DD-affected individuals). We identify hundreds of genes associated with these disorders and reveal significant overlap, as well as substantial heterogeneity, in the genes associated with each phenotype and in the neural cell types expressing them. Overall, these analyses provide new insights into the contributions of rare coding variation in NDDs, including broad overlap and nuanced distinctions of genetic risk and its influence on specific pathways and developmental trajectories.

Results

Patterns of rare coding variants in ASD.

We aggregated exome sequencing data across 33 ASD cohorts that included 63,237 individuals: 15,036 affected probands, 28,522 parents and 5,492 unaffected siblings from

family data, as well as 5,591 affected and 8,597 unaffected individuals from case-control studies (Fig. 1a and Supplementary Tables 1–4). Of the family data, 58.7% had not been published previously. After filtering, variant counts were comparable across cohorts, with an average of 1.64 (1.66 per affected, 1.57 per unaffected) de novo SNVs and 0.18 (0.18 per affected, 0.16 per unaffected) de novo indels per individual. Consistent with previous studies, PTVs and damaging missense variants were enriched in individuals with ASD compared with unaffected individuals (Fig. 1b,c). PTV enrichment was greatest in genes under selective constraint, represented by low LOEUF scores[34] (Supplementary Tables 5–8), with both de novo and inherited PTVs enriched in the lowest three deciles of LOEUF (binomial test; Fig. 1b). We annotated two groups of deleterious missense variants: MisB (MPC ≥ 2) and MisA (2 > MPC ≥ 1); MisB variants were strongly enriched in ASD cases while the effect of MisA variants was modest (Fig. 1c). Overall, we observed the greatest ASD risk in de novo variation, with less significant risk observed in rare case-control (for which de novo status cannot be determined) and inherited variants.

Discovery of rare and de novo CNVs from exome sequencing.

Microarray-based studies have established a clear etiological role for large, rare CNVs in ASD[14,16–18,37–40]. Here, we applied a CNV discovery tool, GATK-gCNV, that predicts read-depth changes from short-read sequencing[41]. We performed extensive benchmarking using orthogonal technologies across 7,035 individuals with matching CNVs detected from WGS[26,42]. These analyses observed 86% sensitivity and a positive predictive value (PPV) of 90% to detect rare (site frequency <1%) CNVs discoverable by WGS at a resolution greater than two captured exons (Fig. 1d), and comparable sensitivity (83%) and PPV (97%) for de novo CNVs (Supplementary Figs. 1 and 2). Using these site frequency and resolution filters, we analyzed CNVs in 55,678 samples with accessible data (Methods; Supplementary Table 4). We observed 17,774 rare inherited and 662 de novo autosomal CNVs after filtering; 3.95% of ASD cases and 1.39% of unaffected siblings harbored at least one de novo coding CNV (odds ratio (OR): 2.91, $P = 2.2 \times 10^{-21}$, Fisher's exact test; Fig. 1e,f and Supplementary Table 9). A greater proportion of female cases harbored de novo CNVs than males (6.0% versus 3.5%, OR: 1.8, $P = 2.1 \times 10^{-8}$, Fisher's exact test), consistent with a female protective effect that proposes a higher burden of risk factors required for an ASD diagnosis in females[17,43]. De novo deletions spanning at least one constrained gene (LOEUF <0.4) showed the greatest enrichment in ASD cases across all variant classes (9.33 fold enrichment, $P = 6.7 \times 10^{-21}$, binomial test), with a relative difference approximately threefold higher than de novo PTVs in the same constraint decile ($P = 2.3 \times 10^{-4}$, permutation test). Duplications showed similar but more attenuated enrichment patterns (Fig. 1e–f).

We next sought to dissect the relative impact of large GD segment CNVs (Fig. 2a) from alterations to individual genes. We considered 79 GD segments previously associated with NDDs, as described in Collins et al.[22]. (Supplementary Table 10). Of the 662 de novo CNVs discovered, 253 (38.2%) matched one of these loci (Methods). As expected, de novo GDs were strongly enriched in ASD cases (deletion OR: 4.8, $P = 2.6 \times 10^{-8}$, duplication OR: 2.9, $P = 3.6 \times 10^{-5}$, Fisher's exact test, Fig. 2b), whereas a weak trend was detected for inherited GDs (OR: 1.2, $P = 0.053$, Fisher's exact test). After excluding GD segments, the remaining

409 de novo CNVs were enriched in ASD probands, but with more modest effect sizes (non-GD deletion OR: 3.1, $P = 1.1 \times 10^{-9}$; non-GD duplication OR: 2.1, $P = 5.4 \times 10^{-4}$, Fisher's exact test). However, the impact of a non-GD de novo deletion of a constrained gene was comparable to a GD deletion (OR: 6.9, $P = 2.2 \times 10^{-12}$, Fisher's exact test, Fig. 2c) and significantly greater than de novo PTVs in constrained genes (OR: 2.74, $P = 3.7 \times 10^{-34}$, Fisher's exact test, Fig. 2c).

We also quantified risk associated with GDs in ASD compared with the general population by applying GATK-gCNV to exome data in the UK Biobank (UKBB)[44]. We processed the UKBB data using identical parameters as the ASD cohort and compared carrier rates for 79 GD loci in 13,786 ASD cases and 145,532 UKBB controls with accessible phenotype information and no documented neuropsychiatric or developmental phenotypes. These analyses demonstrated a linear inverse correlation of decreasing OR in ASD with increasing GD frequency in the UKBB, with the most significant loci including established GDs such as 15q11.2-q13.1, 17q12 and 17q11.2, among others (OR > 50; Fig. 2d). We provide these results in Supplementary Fig. 3 and Supplementary Table 10 as a reference for future GD variant interpretation.

Finally, de novo SNVs and indels arise more frequently on the paternal allele[38,45,46], yet a maternal bias has been observed for de novo CNVs in ASD[47]. We explored the mechanisms associated with this bias using SNV/indel data to estimate the parent of origin for 225 de novo CNVs and observed no bias in ASD cases (Fig. 2e; 49% maternal, $P = 0.89$, binomial test; Methods). However, 69% of de novo CNVs at NAHR-mediated GD loci arose preferentially on the maternal allele ($P = 3.7 \times 10^{-4}$, binomial test) and recapitulated previous findings, with the strongest bias observed for the 16p11.2 CNV across this cohort and the Simons Searchlight project[47,48] (95% maternal origin; Fig. 2e). By contrast, CNVs that were not NAHR-mediated GDs showed a significant paternal bias (63.5%; $P = 2.0 \times 10^{-3}$, binomial test), suggesting a mechanistic maternal bias in NAHR-mediated CNV formation, but a paternal bias in all other classes of de novo SVs, consistent with previous analyses using WGS[42].

Integration of variant classes for ASD gene discovery.

The relative risk of variants associated with ASD varied by mode of inheritance, variant class (PTV, MisB, MisA, deletion and duplication) and evolutionary constraint. We thus sought to leverage these insights to refine ASD gene discovery by extending a Bayesian analytic framework, TADA[4,36], to include (1) rare and de novo CNVs, (2) variants present in unaffected offspring and (3) evolutionary constraint from gnomAD (LOEUF[34], Methods; Supplementary Table 8 and Supplementary Fig. 4). For each autosomal protein-coding gene, a Bayes factor (BF) was calculated to represent evidence of association across variant types and modes of inheritance, taking into account mutation rates and relative risk priors (Fig. 3a).

Applying this model to the aggregated ASD data (TADA-ASD), we identified 72 genes associated with ASD at FDR ≤ 0.001 (Fig. 3b) and 185 genes at FDR ≤ 0.05 (Supplementary Table 11). Within the 72 genes, de novo PTV, MisB or MisA variants were detected in 4.0% of cases and 0.5% of controls (combined OR: 8.44, $P = 3.4 \times 10^{-51}$, Fisher's exact

test), and we applied cross-validation to refine variant class-specific risk (Supplementary Note and Supplementary Table 12). Notably, the FDR ≤ 0.001 used here is approximately equivalent to an exome-wide Bonferroni significance threshold ($P < 2.8 \times 10^{-6}$) when back-calculating a *P* value and correcting for 18,128 autosomal genes, making it comparable with recent studies of schizophrenia[7] and DD[5]. We calibrated the relative impact of the inclusion of multiple variant classes and our updated model parameters here compared with previous ASD studies on a subset of these samples (Fig. 3c and Supplementary Fig. 5). While we observed considerable mutational diversity across ASD risk genes (Fig. 3d,e), haploinsufficiency was the predominant mechanism; PTVs and deletions accounted for greater than 90% of the evidence in 21 of 72 ASD risk genes (29.2%). However, for nine genes (12.5%), greater than 90% of evidence was derived from missense variants and duplications (for example, *DEAF1* and *SLC6A1*; Fig. 4a), including one gene (*PLXNA1*) where overtransmission of missense variants was observed specifically within the Plexin domain of the encoded protein (Fig. 4b,c).

Although this framework is not intended to assess autosomal recessive risk in ASD, we examined offspring with two (or more) PTV and/or MisB alleles within the same gene, whether from homozygous or compound heterozygous variants. We found ten genes with two or more occurrences in ASD cases (*B3GALT6*, *BTN2A2*, *DNAAF3*, *EIF3I*, *FEV*, *KCP*, *RDH11*, *RNF39*, *RNF175* and *SSPO*) and no such occurrence in unaffected siblings. Some genes, such as *FEV*, have been implicated in recessive models of ASD[49], whereas most other genes have not been associated with an autosomal recessive form of ASD and warrant further study.

Lastly, we evaluated two hypotheses regarding the excess burden of de novo variants in females across the 185 FDR ≤ 0.05 genes and the GD loci: (1) the excess is due to a female protective effect; or (2) it arises from an ascertainment bias by which females diagnosed with ASD tend to be affected more severely than males[50]. In fact, both severity and sex are associated with being a carrier of such mutations. Using dichotomized full-scale IQ (FSIQ, 2,095 samples) and autism diagnostic observational scale (ADOS, 5,280 samples) test scores as proxies of phenotypic severity, we constructed logistic regressions to estimate the OR of carrying a de novo damaging variant (PTV, MisB, GD CNV or CNV overlapping one of the 185 ASD genes) as a function of sex and phenotype. We found that ASD individuals harboring these damaging mutations are significantly more likely to be female and to be severely affected, and that sex and severity status combined additively to determine burden. There was no evidence of an interaction effect, which would be expected with ascertainment bias (Methods; Supplementary Table 13a–d). Thus, these analyses strongly favor the female protective effect.

Comparing the genetic architectures of ASD and general DD.

Significant overlap has been observed between genes affecting ASD and those affecting development more broadly, including NDDs[51,52]. To explore commonalities and differences across genes that impact NDD risk, we sought to integrate data from our ASD cohort with an independent cohort of 31,058 offspring ascertained for broadly defined DD and their parents[5]. De novo SNVs and indels from this cohort were analyzed recently using

DeNovoWEST, a permutation-based frequentist method, which reported association for 252 autosomal genes[5]. We reanalyzed these data using our TADA framework to enable direct comparisons between cohorts using uniform statistical models and significance thresholds. This implementation identified 309 autosomal genes associated at FDR ≤ 0.001 (TADA-DD), including 237 (94%) of the 252 autosomal genes discovered previously[5] (Supplementary Table 11). Moreover, our FDR values were highly correlated with those derived from the DeNovoWEST significance values[5] ($r = 0.95$, $P < 1.0 \times 10^{-22}$; Supplementary Fig. 6). As expected, given the enrichment of cases with severe and syndromic disorders in the DD cohort[5], the de novo PTV, MisB and MisA counts in offspring showed similar but much stronger variant enrichment across the top three deciles of LOEUF (Fig. 5a,b).

Because a cardinal rule of meta-analysis is that the data should not be too heterogeneous, before combining results across cohorts, we assessed whether the genes identified in the ASD cohort were also associated in the DD cohort, and vice versa. To do so, we converted the distribution of TADA FDRs to *P* values for each study (Methods). If the genes associated in one cohort were also associated in the other, or some fraction thereof, the distribution of their association *P* values would be skewed toward zero. When we selected the 477 genes associated in the DD cohort from the TADA-DD analysis at FDR ≤ 0.05, the estimated fraction of ASD genes also showing association was 0.701 (Methods; Fig. 5c), indicating that 70.1% of these DD genes affect risk for ASD. The converse conditioning estimated that 86.6% of ASD risk genes have broad effects on development (Fig. 5c,d). Thus, because the ASD and DD cohorts are somewhat complementary, we conducted a joint analysis using the TADA framework to integrate the genetic evidence for each gene across the cohorts by combining the BFs, conceptually similar to a frequentist meta-analysis. This combined analysis (TADA-NDD) revealed 373 genes associated with general NDDs at FDR ≤ 0.001 (664 genes at FDR ≤ 0.05; Supplementary Table 11). Notably, 54 of the 373 genes did not achieve FDR ≤ 0.001 in either cohort alone, demonstrating a 14% increase in yield. Although we did not have access to CNV data from the DD cohort, we nonetheless found a profound and specific enrichment of 134 de novo CNVs that impacted one of the 373 TADA-NDD genes across all ASD cases and only one such CNV in siblings (OR: 48.9, $P = 6.4 \times 10^{-17}$, Fisher's exact test). We also used this set of genes to assess support for an oligogenic model of ASD and DD, finding no support for the hypothesis (Methods; Supplementary Tables 14a–c).

Heterogeneity of mutation patterns between ASD/DD risk genes.

Isolating genes that exert a greater effect on ASD than they do on other DDs has remained challenging due to the frequent comorbidity of these phenotypes. Still, an estimated 13.4% of the TADA-ASD genes show little evidence for association in the DD cohort (Fig. 5d). The remainder are likely pleiotropic, yet some could have a greater impact on ASD risk than other features of development. To evaluate heterogeneity between the ASD and DD cohorts, we retained only de novo SNVs/indels for independent gene-level BF calculations. For the 373 genes at TADA-NDD FDR ≤ 0.001, we observed a Pearson's correlation of 0.78 of the gene-level log BF between the two main ASD subcohorts (the Simons Powering Autism Research (SPARK) initiative versus all others) compared with 0.42 between the ASD and

DD cohorts, reflecting more consistent evidence between ASD cohorts than between ASD and DD cohorts (Supplementary Fig. 7).

We next determined which genes were more commonly mutated in one cohort or the other by selecting 464 'signal genes' (Supplementary Table 15). These genes were defined as any gene with FDR ≤ 0.05 in either TADA-ASD or TADA-DD from de novo PTVs and MisB variants, which as classes confer similar relative risk for ASD (Fig. 1b,c); MisA variants were excluded because they conferred far less risk (Fig. 1b,c). Of these signal genes, 120 belonged to TADA-ASD, 428 to TADA-DD and 84 to both. Notably, the 84 genes significant in both cohorts still demonstrated significant variant count heterogeneity ($\chi^2 = 317.6$, d.f. = 83, $P = 3.8 \times 10^{-23}$) between the cohorts. A common way to assess which of the 464 genes have more variation in either cohort would be a standardized C statistic (Methods), but its power to discriminate is abrogated by the much higher burden of risk variants in the DD cohort (Fig. 5a,b). We therefore adjusted for the difference in mutational burden between the cohorts by randomly downsampling the DD mutations to be comparable to that for ASD mutations. A mixture model was then adopted to disentangle the two commingled distributions, assigning posterior probabilities that a gene is from the ASD or DD component of the statistical distribution (Fig. 5e,f and Supplementary Table 15). Using a posterior probability cutoff of greater than 0.99, we find 36 genes to be a part of the ASD mixture component (ASD-predominant) and 82 genes to be a part of the DD component (DD-predominant) (Fig. 5f and Supplementary Table 15).

Differential neuronal layers impacted by ASD/DD risk genes.

To explore differences in expression between genes identified across ASD and DD cohorts, we examined single-cell gene expression patterns from human fetal brains. Two studies provided data from more than 37,000 cortical cells ranging from 6 to 27 weeks postconception[53,54] (Supplementary Table 16). To combine these datasets, we adjusted for batch effects using cFIT[55]. Uniform manifold approximation and projection (UMAP) plots showed that similar cell types from the different batches grouped together, while cells unique to either batch were preserved (Fig. 6a and Supplementary Fig. 8). We applied unsupervised clustering to the combined data to identify cell subtypes in the context of a hierarchical tree to illustrate the relationships between major and minor cell type clusters. Using the MRtree method[56], we observed that cells of each labeled type were merged across datasets into common clusters. Visualizing the tree, the main branches corresponded to glial and progenitor cells, excitatory neurons, deep layer enriched excitatory neurons and inhibitory neurons (Supplementary Table 17). Likewise, minor splits reflected expected relationships between cell types (Supplementary Fig. 9a). Based on the trajectory analysis of Polioudakis et al.[57], the ExN clade is less differentiated than the ExM clade, which in turn is less differentiated than the ExMU clade.

Next, we assessed the enrichment of ASD and DD risk genes meeting the posterior probability 0.99 threshold within cell clusters (Fig. 5f). Among the 36 genes classified as ASD-predominant, 22 were expressed in these cell types; of the 82 genes classified as DD-predominant, 59 were expressed. Using ORs to reflect the strength of signal, both ASD-predominant and DD-predominant genes were enriched in interneurons and excitatory

neurons compared with glial and progenitor cells (Fig. 6b, Supplementary Fig. 10 and Supplementary Tables 15, 18 and 19). ASD-predominant enrichment seemed somewhat stronger than DD-predominant enrichment in excitatory neuron lineages, with a difference in log-odds values (comparing enrichment in the main clade of excitatory neurons to progenitors) of 1.29 for ASD and 0.7 for DD (one-sided $P = 0.017$ for ASD; $P = 0.031$ for DD).

The DD-predominant expressed genes tend to occur in cell types that are less differentiated than the corresponding cell type enriched for ASD-predominant genes: ExN3, ExM2, IP, InCGE (for details, see Supplementary Table 18 and Supplementary Note). By contrast, ASD-predominant expressed genes (Supplementary Table 19) are strongly enriched in only one cell type, maturing excitatory neurons (ExMU1) and its clade. These genes highlight a shift from mainly migration-focused genes to more mature processes involved in building the neurons' nascent connectivity. If we judge enrichment solely by significance after Bonferroni correction for 21 cell types, ExMU1 remained significant for enrichment of ASD-predominant genes; likewise, ExN3 remained significant for enrichment of DD-predominant genes. Our results are consistent with DD-predominant genes being expressed earlier in development and in less differentiated cells than ASD-predominant genes.

Emergence of shared risk genes in schizophrenia and ASD.

Shared genetic risk between ASD and schizophrenia, as well as other neuropsychiatric disorders, has long been postulated[54]. The Schizophrenia Exome Meta-Analysis (SCHEMA) Consortium recently identified 244 genes associated with schizophrenia at $P < 0.01$ (ref. [7]), 234 of which are in our TADA model. Among the 72 ASD genes we discovered at FDR ≤ 0.001, 61 were associated with DD (using TADA-DD FDR ≤ 0.001), and 8 were associated with schizophrenia at $P < 0.01$. These two groups of 61 ASD/DD genes and 8 ASD/schizophrenia genes overlap each other less than expected ($P = 0.023$, binomial test; Methods; Supplementary Fig. 11a). Similarly, using the gene sets shown in Fig. 5f, 6 of the 36 ASD-predominant genes (*ANK2*, *ASH1L*, *BRSK2*, *CGREF1*, *DSCAM* and *NRXN1*) are schizophrenia-associated, while only 3 of the 82 DD-predominant genes (*ATP2B1*, *GRIN2A* and *HIST1H1E*) are schizophrenia-associated. The ASD-schizophrenia overlap was significantly enriched ($P = 8.4 \times 10^{-6}$, binomial test), while the DD-schizophrenia overlap was not ($P = 0.10$, binomial test; Methods; Supplementary Fig. 11b). The two outcomes (6/36 versus 3/82) were also different when compared with each other ($P = 0.023$, Fisher's exact test). Together, these data suggest that one subset of ASD risk genes may overlap DD while a different subset overlaps schizophrenia.

Discussion

Integrating rare protein-coding SNVs, indels and CNVs across 63,237 individuals from ASD cohorts reveals an allelic spectrum of rare coding variation associated with ASD that is dominated by de novo PTVs, damaging missense variants and deletions of constrained genes. Nonetheless, many genes were associated with multiple inheritance or variant classes and some showed the strongest evidence from de novo missense variants and duplications. While discovery is currently driven by de novo variants imparting loss of function, larger

ASD cohorts will likely catalyze future discoveries from the subtler and more heterogeneous functional effects of missense variants and intragenic or individual exon duplications. Independently applying the same statistical model to both the DD and ASD datasets reinforces that our analytic framework and statistical thresholds are robust, as our results for DD are highly correlated with the permutation-based approach applied to those same data[5]. Integrating the two cohorts together yielded 373 genes at FDR ≤ 0.001, including 54 genes that were unique to the joint analyses and were not captured by either dataset alone, and 664 likely risk genes at FDR ≤ 0.05.

This study, at the time of analysis, is also the largest exploration so far of CNVs at the resolution of individual genes and exons to ASD architecture. Benchmarking against WGS, more than 85% of all rare coding CNVs spanning more than two exons could be recalled by exome-based CNV discovery. We find that deletion of a highly constrained gene confers comparable risk to alteration of an established GD segment, and we observe a dramatic enrichment of CNVs among ASD probands compared with unaffected siblings across the 373 NDD risk genes identified. We also recapitulate the observation of a maternal bias in gamete-of-origin for de novo CNVs in ASD probands[47] but find this enrichment to be restricted to NAHR-mediated CNVs (for example, 95% of 16p11.2 CNVs), whereas all other mechanisms were predominantly paternal in origin and consistent with previous WGS analysis in controls[42]. These results collectively emphasize the value of routine joint analysis of all classes of genomic variation in gene discovery and the potential impact of gene-level CNV analyses in diagnostic testing.

We expect these findings to shed light on the neurobiological origins of ASD. However, given the substantial overlap between the genes implicated in NDDs writ large and those implicated directly in ASD, disentangling the relative impact of individual genes on neurodevelopment and phenotypic spectra is a daunting yet important challenge. Consider two of the ASD risk genes: *ARID1B* and *DSCAM*. Both are highly associated with ASD, although statistical evidence is stronger for *ARID1B*. Yet while some individuals with mutations in *ARID1B* also have comorbid ASD, it is only one of a wide range of developmental phenotypes[58]. The profound impact of *ARID1B* on development is apparent by the contrast of de novo mutations in the DD and ASD cohorts: 132 carriers out of 31,058 DD probands versus 9 carriers out of 15,036 ASD probands, a sevenfold higher rate in DD. This raises a challenge for neurobiologists: neurodevelopmental features associated with perturbation of *ARID1B* could be relevant to DD, yet irrelevant to ASD. Because evidence for *DSCAM* comes solely from the ASD cohort, it could be a better choice for neurobiological studies of ASD. Still, as we develop here, *DSCAM* is also involved in risk for schizophrenia, and studies such as ours continue to demonstrate the pleiotropic consequences of many such genes implicated in ASD and NDD risk. To identify the key neurobiological features of ASD will likely require convergence of evidence from many ASD genes and studies. Careful selection of candidates among the genes implicated here based on their mutational and functional features could inform these future studies. We have taken a step in that direction, as genes expressed at earlier stages of cortical development, such as progenitor genes, broadly show greater DD enrichment, while those expressed later, such as maturing neurons, lean towards ASD. This is consistent with the expectation that earlier and more generalized impairment leads to severe global DD while later, neuron-

specific impairment affects more isolated developmental domains, such as social interaction and the presence of repetitive behaviors and/or interests that typify ASD.

In conclusion, our analyses of rare coding variation illuminate the allelic diversity contributing to ASD and both the shared and distinct genetic architectures between ASD and related NDDs. We further highlight enrichment of associated genes at different neuronal timepoints. The consortia studies aggregated here have catalyzed a rapid evolution in genetic studies in ASD, including preliminary analyses in recent preprints that have leveraged these data for insights into gene discovery in ASD and DD datasets, and into the combined impact of rare and common variant polygenic risk across males and females[8,9,59,60]. As sample sizes rapidly expand, the analytic framework presented here will continue to yield returns in both gene discovery and improved understanding of the differential risks to disorders on the neurodevelopmental and neuropsychiatric spectrum posed by variants within these genes.

Online content

Any methods, additional references, Nature Research reporting summaries, source data, extended data, supplementary information, acknowledgements, peer review information; details of author contributions and competing interests; and statements of data and code availability are available at https://doi.org/10.1038/s41588-022-01104-0.

Methods

We confirm that this research complies with all relevant ethical regulations and was approved by the Mass General Brigham Human Research Committee (MGBHRC) Institutional Review Board (IRB): Study Protocol 2012P001018, The Study of Novel Autism Genes and Other Neurodevelopmental Disorders (12 March 2021) and Study Protocol 2013P000323, Genomic Studies of Human Neurodevelopment (7 September 2018).

Protocols undergo annual continuing review by the MGBHRC IRB (Mass General Brigham, 399 Revolution Drive, Suite 710, Somerville, MA 02145, USA). All necessary patient/participant consent has been obtained and the appropriate institutional forms have been archived. No participant compensation was provided from this study.

SNV/indel processing.

ASD samples were aggregated from four independent sources: (1) previously published data from the Autism Sequencing Consortium (ASC; total $n = 26,268$ (refs. [4,61])); (2) previously published data from the Simons Foundation Autism Research Initiative (SFARI) Simons Simplex Collection (SSC; total $n = 9,170$ (refs. [61,62])); (3) unpublished data from the ASC ($n = 5,036$) and (4) the recently released Simons Foundation Powering Autism Research for Knowledge (SPARK initiative; $n = 22,766$ (ref. [63])). The distribution of these samples is provided in Supplementary Table 1 (one family is in both SPARK and unpublished ASC data, with different probands; one mother in the unpublished ASC data is also a proband in a different trio in the same dataset).

From these sources, family-based samples were processed and genotyped jointly in four batches. The first two batches included the published and unpublished ASC and SSC cohorts: (1) 'ASC B14' included ASC samples through consortium sequencing batch 14 plus the SSC (n = 24,099; 4,632 new; 14,415 males and 9,684 females); (2) 'ASC B15–16' included ASC batches 15 and 16 (n = 832, all new, 500 males and 332 females). The following two batches included two independent releases of the SPARK cohort: (3) the 'SPARK Pilot' initial release (n = 1,379; 833 males and 546 females) and (4) the SPARK.27k.201909 ('SPARK main freeze') release (n = 21,387; 12,679 males and 8,708 males).

Raw sequencing outputs were aligned where needed to the GRCh38 reference genome and variants were jointly called following GATK[64] best practices. Briefly, individual gVCFs were generated by GATK HaplotypeCaller in gVCF mode and subsequently jointly genotyped for high confidence alleles using GenotypeGVCFs, accompanied by variant quality score recalibration to produce output VCFs. For additional details containing the specifics for each of the four batches, please see Supplementary Note. Finally, raw data were not available for 1,354 children and family members reported in Satterstrom et al.[4], and these variants were lifted over directly to GRCh38 (Supplementary Table 1).

SNV/indel filtering.

Creation of working datasets.—Hail v.0.2 (https://hail.is) was used to process VCFs and write working datasets. Reported relationships and sample uniqueness were verified, sex was imputed and variant consequences were annotated. Genotypes were filtered based on (1) depth, (2) genotype quality, (3) phred-scaled likelihood of the call being homozygous reference (PL[HomRef]), (4) allele balance, (5) number of informative reads and (6) Hardy–Weinberg P value. For additional details, see Supplementary Note.

De novo variant calling and quality control.—For curation of de novo variants, we used Hail's de_novo() function to identify candidate variants, taking into account population variant frequencies. Candidates were further filtered based on: (1) frequency in gnomAD population and within their respective dataset, (2) 'ExcessHet' filter, (3) allele balance and parent/child depth ratio, (4) variant quality score log-odds values and (5) excess number of de novo candidate variants within the same sample. For additional details, see Supplementary Note.

Case-control variants.—ASC case-control samples consisted of Danish iPSYCH samples and Swedish PAGES samples. Rare variant counts for 4,863 autism and 5,002 control samples from the iPSYCH cohort were taken from the data of Satterstrom et al.[65], where rare variants were defined as those with an allele count no greater than five in the combination of the iPSYCH data with non-Finnish Europeans from the nonpsychiatric subset of gnomAD (a total of 58,121 people). In addition to samples labeled as 'Autism,' samples labeled as 'Both' in that study (meaning that an individual had both autism and ADHD diagnoses) were used as autism cases for our purposes. Rare variant counts for 728 autism and 3,595 control samples from the PAGES cohort were taken from Satterstrom et al.[4], where rare variants were defined as those with an allele count no greater than five in

the 18,153 combined parents, cases, and controls in the dataset, as well as an allele count no greater than five in the nonpsychiatric subset of ExAC r0.3 (45,376 people). Counts were removed for 17 cases for whom parental sequences became available, so that they are now included in our family-based data instead.

Transmitted variants.—Counts of transmitted and nontransmitted alleles were produced starting from each of the four working datasets described above. First, variants were dropped that had been marked 'ExcessHet' in the Filters field by GATK or had allele frequencies greater than 0.1% in either their own dataset or the nonneuro subset of gnomAD GRCh38 exomes v.2.1.1. In addition, a filter requiring a genotype quality of at least 25 was applied to every genotype. Hail's transmission_disequilibrium_test() function was then called to count transmitted and untransmitted alleles for each variant in family-based data. Subsequently, additional dataset-specific filters on variant quality score log-odds values were applied to derive final counts of transmitted and nontransmitted alleles. For additional details, see Supplementary Note.

CNV processing.

For the subset of samples with available raw genomic data (Supplementary Table 3), we employed GATK-gCNV for exome CNV detection, along with an additional supplement of 7,832 general research use controls. GATK-gCNV is a Bayesian method specifically designed to adjust for known bias factors in exome capture and sequencing (for example, GC content), while automatically controlling for other technical and systematic differences. Briefly, raw sequencing files were compressed into read counts over the set of annotated exons and used as input, and a principal component analysis-based approach was implemented on observed read counts to distinguish differences in capture kits (Supplementary Fig. 1), followed by a hybrid density- and distance-based clustering approach to curate batches of samples for parallel processing. After batching determination, GATK-gCNV was run for each batch and filtering metrics produced by the underlying Bayesian model were used to balance between sensitivity and PPV. For details, see Supplementary Note. Of note, we observed five instances among probands of possibly complex de novo SVs on chromosome 15, exhibiting adjacent GD duplications of differing copy states (Supplementary Table 9).

CNV benchmarking.

We had access to 8,439 samples for which matching genome and exome sequencing data were available for benchmarking comparisons. The ground truth data were CNVs called from WGS using the ensemble machine learning method GATK-SV[25,26]. After removing samples that did not pass GATK-gCNV exome QC filters (Supplementary Note, $n = 971$ samples) and removing samples that had an outlier number of rare (site frequency <1%) calls in the GATK-SV genome callset (>16 rare calls, based on median + 2 × interquartile range, $n = 477$ samples), 7,035 samples remained for direct comparison. Benchmarking was carried out for all rare CNVs (site frequency <1%). Sensitivity was measured by the proportion of sites called from WGS data that had a match in the GATK-gCNV callset. Specifically, for each site, if at least 50% of the samples that had that CNV in the WGS data also had a GATK-gCNV call with a consistent direction (deletion or duplication) that

overlapped at least 50% of the captured intervals, this was considered a success. For CNVs called by GATK-gCNV, PPV was measured by requiring that 50% of the GATK-gCNV samples with that call had a match in the WGS calls (ground truth) with at least 50% interval overlap. We evaluated sensitivity and PPV as a function of the number of captured exons overlapping the canonical transcripts of protein-coding genes.

TADA Bayesian framework for gene association.

TADA is a Bayesian framework that produces gene-level measures of evidence for association that can be transformed into a FDR[42]. Broadly speaking, for a given variant type and gene, TADA produces a BF to measure statistical evidence, taking as input the count of variant events, the mutation rate, the number of samples and a prior on the risk of a variant in each gene. BF can be readily combined across different variant types for the same gene by multiplication, arriving at a total measure of association for a given gene. This total BF can then be transformed directly into a FDR and the appropriate statistical threshold can be applied to extract a candidate gene list. In the previous TADA study[4], evidence was aggregated for de novo PTVs, MisB variants and MisA variants, as well as case/control PTVs to find 102 genes meeting an FDR ≤ 0.1 threshold.

For this analysis, we extended TADA to leverage updated measures of constraint (LOEUF) and the full combination of de novo, case/control and inherited × PTV, MisB, MisA, deletion and duplication variants, as well as variants in unaffected siblings. For full details, see Supplementary Note.

Applying TADA to DD data.

We accessed the summary tables released by the DDD in Kaplanis et al.[5], detailing de novo variants detected and gene-level variant counts in 31,058 trios where the offspring was diagnosed with a developmental disorder. To calculate the number of PTVs per gene, we aggregated the Kaplanis et al. variants annotated with consequences of ‘frameshift_variant,’ ‘splice_donor_variant,’ ‘splice_acceptor_variant’ or ‘stop_gained.’ For synonymous counts, we aggregated variants with labels of ‘synonymous_variant’ or ‘stop_retained_variant.’ We annotated missense variants (‘missense_variant’) with MPC scores and, using those MPC scores, we assigned MisB and MisA status and aggregated counts per gene.

To create TADA-DD, we supplied the per-gene counts of PTVs, MisA variants and MisB variants to TADA in the same manner as we supplied our ASD cohort counts. TADA-DD BFs were then combined with those from the ASD cohort on a per-gene basis, allowing us to estimate FDR on a combined NDD super-cohort (TADA-NDD).

Comparison of TADA-DD and denovoWEST data from Kaplanis.—Kaplanis et al.[5] report association values for 19,654 genes, of which 285 are significant at an exome-wide threshold. Of the 18,128 autosomal genes investigated by our study, 17,919 (99%) have a match from Kaplanis et al., including all 252 significant autosomal genes. Of the Kaplanis et al. denovoWEST exome-wide significant genes, 237/252 (94%) are also found in the TADA-DD FDR ≤ 0.001 list.

We also measured the concordance of the Bayesian TADA-DD FDR with the most frequent denovoWEST estimates of gene significance reported in Kaplanis et al.[5] by transforming the Kaplanis *P* values (denovoWEST_p_full) into FDRs (FDR denovoWEST) using the R function p.adjust(method = 'fdr'). A pairwise plot of TADA-DD FDR with transformed Kaplanis FDR reveals high concordance (Supplementary Fig. 6; cor = 0.95) on the log scale, signaling convergence in evaluation of gene-level evidence between our studies, and allowing us to integrate the Kaplanis variant data into our Bayesian framework.

Female protective effect versus ascertainment bias of affected females.

Severity of phenotype and sex are known to be associated with the presence of de novo SNV/indel or CNV mutations in individuals with ASD. Specifically, those with more severe phenotypes or females are more likely to be carriers of such mutations. Notably, various studies have also found that females are less likely to be diagnosed with ASD compared with males with similar presentation[50,66,67], creating the possibility that the excess burden of damaging de novo variants observed in females could be due to this ascertainment bias—females are simply more severely affected. An alternative is that severity and sex combine approximately additively to determine burden. This would be consistent with an alternative hypothesis—a female protective effect—that posits that females require a greater burden of genetic risk variation to be affected. Using ADOS and IQ as proxies for severity where available, we constructed logistic regression models of carrier status as the outcome and sex, severity and their interactions as predictors. We found no evidence to support ascertainment bias and instead favor the additive alternative (Supplementary Table 13). For more details, see Supplementary Note.

Evaluating oligogenicity in ASD and DD.

We tabulated the number of individuals with zero, one and two de novo damaging variants (PTV or MisB) among the TADA-ASD 72, TADA-ASD 185, and TADA-NDD 373 genes and constructed a Poisson expectation on the number of expected individuals with two such variants as follows:

$$p = (\text{number of variants/number of samples})^2$$
$$\text{Expectation} = (p \times \text{ number of samples }) \times \exp(-p)/2!$$

These analyses also offer a glimpse into the evidence supporting an oligogenic model of ASD and DD. Using the list of 373 NDD-associated genes, we observed 913 (6.1%) of the 15,036 ASD probands harboring a damaging de novo variant of interest (PTV or MisB), and 12 probands that carried two (0.08%). Across all 31,058 DD probands, one de novo variant was found in 5,176 (16.7%) cases, and 96 (0.31%) carried two. Using a Poisson expectation model for the number of affected individuals carrying two variants, we find depletion in both the ASD and DD cases carrying two variants (ASD: 27.4 expected, 12 observed; DD: 390 expected, 96 observed). This same depletion was observed when restricting to the 72 or 185 genes associated with ASD alone, indicating no support for oligogenicity among ASD or DD cases from these analyses (Supplementary Tables 14a–c).

Conditional analysis of cross-cohort association.

For the ASD and DD cohorts, separately, we first converted the set of 18,128 gene *q*-values into *P* values using the following R command: pval = qval × rank(qval) / (max(qval) × length(qval)). Next, we selected genes meeting FDR ≤ 0.05 from the TADA-ASD and TADA-DD cohorts, treating the derived lists separately. For the set of 185 identified TADA-ASD genes, we evaluated the distribution of their back-transformed *P* values from TADA-DD using the 'propTrueNull' function from the R package limma_3.38.3 (refs. [68,69]) to estimate pi0 and pi1 = 1 − pi0, which is the estimated fraction of the number of genes associated in the DD cohort. pi0 is the estimated fraction of genes that have no association and for which their *P* values would be distributed uniformly on the interval 0 – 1. We then did the converse: choosing the set of 477 identified TADA-DD genes, we evaluated the distribution of their *P* values from TADA-ASD to estimate pi1.

ASD-DDD heterogeneity analysis.

We asked which of the 464 signal genes was more tightly connected with either ASD or DD than expected by chance. To do so, we formulated an approach that builds on the familiar chi-statistic residual. Before computing the residuals, we needed to overcome the far larger number of mutations present in the DD sample because the standardized residual performs best when the total count of events, per cohort, is equal. We therefore down-sampled the DD mutations in signal genes to obtain a count of 1,001 mutations, matching the count of mutations in the ASD cohort. This was repeated 100 times.

C statistic.—For the C statistic, we used a standard log-linear model analysis by conditioning on the row (gene) and column totals (over ASD or DDD). We asked if the residual for ASD was substantially different from that expected under the null. The residual for gene *i* was defined as:

$$C_i^{\mathrm{ds}} = \frac{\left(\mathrm{dn.asd}_i^{\mathrm{obs}} - \mathrm{dn.asd}_i^{\mathrm{exp}}\right)}{\sqrt{\mathrm{dn.asd}_i^{\mathrm{exp}}}}$$

where:

$$\mathrm{dn.asd}_i^{\mathrm{exp}} = \mathrm{dn}^2.\mathrm{asd}_i^{\mathrm{obs}} \times \left(\mathrm{dn}^2.\mathrm{asd}_{\mathrm{i}}^{\mathrm{obs}} + \mathrm{dn.ddd}_i^{\mathrm{obs}}\right)/N$$

with the average over the 100 downsampling repetitions recorded as the C statistic for each gene.

Mixture modeling.

If gene mutation rates were independent of cohort, then the C statistic would be distributed as a standard normal statistic, but this was clearly not true (Fig. 5e). Genes with unusually few mutations in the ASD cohort produced a negative C statistic and those with unusually many mutations in the ASD cohort produced a positive statistic. Assuming the genes split into two classes, one favoring DD mutations and the other favoring ASD mutations, we

fitted a two-component normal mixture model. This calculation was performed using the normalmixEM function in the 'mixtools' R package[70]. We restricted the model to have a common s.d. for both components (option arbvar = F), which was estimated to be 0.527. Although the C statistics varied continuously across the spectrum of values observed, we could estimate the posterior probability a gene was from the DD or ASD component to determine likely group membership. Genes with posterior probability greater than 0.99 for either class were labeled by that class.

Tree analysis.

To understand the developmental cell types in which these genes were expressed, we analyzed two datasets using a new approach called cFIT, the common factor integration and transfer learning algorithm[55]. cFIT relies on a linear model assuming a common factor matrix shared among datasets, as well as gene-wise location and scale shifts unique to each dataset. It estimates the shared and batch-specific parameters through iterative nonnegative matrix factorization and then recovers the batch-free expression for each dataset based on the common factor and factor loadings. We applied cFIT to fetal cells from two studies[53,57] and used unsupervised clustering (MRtree)[56] to the integrated data to generate a hierarchical tree of various cell types. For details, see Supplementary Note.

Enrichment analysis.

We performed enrichment analysis for each cluster in the resulting tree to determine if any clusters expressed an unusual number of ASD-predominant or DD-predominant risk genes. Before performing the enrichment analysis, that is, creating a 2 × 2 table for expressed gene (yes/no) by risk gene (yes/no), we needed to first identify the set of genes to be included in the analysis, which is defined as the set of genes 'expressed' in at least one cell type. Because the integration process often replaces zero values in the gene expression matrix with small positive values, we considered any integrated expression value less than 0.5 to be nonexpressed. A gene was considered 'expressed' for a particular cell type if its expression was greater than 0.5 for at least 25% of the cells in the terminal clusters. For each cluster, we then determined if the expressed genes belonged to the ASD-predominant or DD-predominant gene sets and computed the OR from the 2 × 2 table to determine enrichment (Fig. 5c).

Evaluating overlap with schizophrenia-associated genes.

We compared our ASD- and DD-associated genes to the schizophrenia-associated genes reported by SCHEMA[7] to determine if there was any overlap between ASD and schizophrenia at the level of individual risk genes and, if so, whether it was related to ASD-DD overlap. Note that 3 out of 309 genes with FDR ≤ 0.001 in TADA-DD were not included in the SCHEMA results, while 10 out of 244 genes identified by SCHEMA as schizophrenia-associated at $P < 0.01$ were not evaluated by our TADA model (8/10 were on chromosome X).

As described in the main text, among the 72 ASD genes we discovered at an FDR ≤ 0.001, 61 show an association with DD (using FDR ≤ 0.001, based on TADA-DD), and 8 show an association with schizophrenia at $P < 0.01$. If the two associations were independent, we

would expect roughly one of the eight ASD-schizophrenia genes to lack an association with DD (based on all but 11/72 = ~15% of the ASD genes overlapping DD). However, we in fact find that four of the ASD-schizophrenia genes lack an association with DD, which is a significant overrepresentation compared with random chance ($P = 0.023$, binomial test; Supplementary Fig. 11a).

We also analyzed ASD-schizophrenia overlap using the 36 ASD-predominant genes and 82 DD-predominant genes shown at the extremities of the distribution in Fig. 5f (which shows posterior probability for ASD enrichment of the genes in our heterogeneity analysis). We looked for overlap between these gene sets and the 244 genes identified by SCHEMA as schizophrenia-associated at $P < 0.01$. We found that 6 of the 36 ASD-predominant genes were schizophrenia-associated, while 3 of the 82 DD-predominant genes were schizophrenia-associated (Supplementary Fig. 11b). If we compare with the null hypothesis that each of the 17,294 genes from our TADA model that are also in the SCHEMA results has an equal chance of being schizophrenia-associated, then the ASD-schizophrenia overlap is significantly enriched ($P = 8.4 \times 10^{-6}$, binomial test), while the DD-schizophrenia overlap is not ($P = 0.10$, binomial test). The two outcomes (6/36 versus 3/82) are also different when compared with each other ($P = 0.023$, Fisher's exact test).

Reporting summary.

Further information on research design is available in the Nature Research Reporting Summary linked to this article.

Data availability

The data used in this study are available at: Repository/DataBank Accession: NHGRI AnVIL; accession ID: phs000298; Databank URL: https://anvilproject.org/data; Repository/DataBank Accession: Simons Foundation for Autism Research Initiative SFARIbase; accession ID: SPARK/Regeneron/SPARK_WES_2/; Databank URL: https://www.sfari.org/resource/spark/; de novo variant data used analyses reported in Supplementary Table 9 (CNVs) and Supplementary Table 20 (SNV/indels). Other candidate de novo CNVs that were either too small (spanning two exons or less) or did not meet quality score threshold (quality score < 200) to be included in our statistical analyses are reported in Supplementary Table 21. Aggregated rare variant counts (inherited, case/control) are released in Supplementary Tables 5–7. To access all individual variants, please see above repositories. GRCh38 reference genome: gs://gcp-public-data–broad-references/hg38/v0/Homo_sapiens_assembly38.fasta; Access to UK Biobank data will be provided by the UK Biobank.

Code availability

The R code used to generate TADA association results is available under the MIT license at https://github.com/talkowski-lab/TADA_2022; https://doi.org/10.5281/zenodo.6496480; analyses executed in R 3.5.3: limma_3.38.3, stringr_1.4.0, GenomicRanges_1.34.0, GenomeInfoDb_1.18.1, IRanges_2.16.0, S4Vectors_0.20.1 and BiocGenerics_0.28.0.

Supplementary Material

Refer to Web version on PubMed Central for supplementary material.

Authors

Jack M. Fu[1,2,3,82], F. Kyle Satterstrom[2,4,5,82], Minshi Peng[6,82], Harrison Brand[1,2,3,7,82], Ryan L. Collins[1,2,3,8], Shan Dong[9], Brie Wamsley[10], Lambertus Klei[11], Lily Wang[2,8], Stephanie P. Hao[1,3,7], Christine R. Stevens[2,4,5], Caroline Cusick[4], Mehrtash Babadi[12], Eric Banks[12], Brett Collins[13,14,15], Sheila Dodge[16], Stacey B. Gabriel[16], Laura Gauthier[12], Samuel K. Lee[12], Lindsay Liang[9], Alicia Ljungdahl[9], Behrang Mahjani[13,14,17], Laura Sloofman[13,14,15], Andrey N. Smirnov[12], Mafalda Barbosa[15,18], Catalina Betancur[19], Alfredo Brusco[20,21], Brian H. Y. Chung[22], Edwin H. Cook[23], Michael L. Cuccaro[24], Enrico Domenici[25], Giovanni Battista Ferrero[26], J. Jay Gargus[27], Gail E. Herman[28], Irva Hertz-Picciotto[29], Patricia Maciel[30], Dara S. Manoach[31], Maria Rita Passos-Bueno[32], Antonio M. Persico[33], Alessandra Renieri[34,35,36], James S. Sutcliffe[37,38], Flora Tassone[29,39], Elisabetta Trabetti[40], Gabriele Campos[32], Simona Cardaropoli[26], Diana Carli[26], Marcus C. Y. Chan[22], Chiara Fallerini[34,35], Elisa Giorgio[20], Ana Cristina Girardi[32], Emily Hansen-Kiss[41], So Lun Lee[22], Carla Lintas[42], Yunin Ludena[29], Rachel Nguyen[27], Lisa Pavinato[20], Margaret Pericak-Vance[24], Isaac N. Pessah[29,43], Rebecca J. Schmidt[29], Moyra Smith[27], Claudia I. S. Costa[32], Slavica Trajkova[20], Jaqueline Y. T. Wang[32], Mullin H. C. Yu[22],
The Autism Sequencing Consortium (ASC)*,
Broad Institute Center for Common Disease Genomics (Broad-CCDG)*,
iPSYCH-BROAD Consortium*,
David J. Cutler[44], Silvia De Rubeis[13,14,15,45], Joseph D. Buxbaum[13,14,15,18,45,46,✉], Mark J. Daly[1,2,4,5,47,48,✉], Bernie Devlin[11,✉], Kathryn Roeder[6,49,✉], Stephan J. Sanders[9,✉], Michael E. Talkowski[1,2,3,4,8,✉]

Affiliations

[1]Center for Genomic Medicine, Massachusetts General Hospital, Boston, MA, USA.

[2]Program in Medical and Population Genetics, Broad Institute of MIT and Harvard, Cambridge, MA, USA.

[3]Department of Neurology, Massachusetts General Hospital and Harvard Medical School, Boston, MA, USA.

[4]Stanley Center for Psychiatric Research, Broad Institute of MIT and Harvard, Cambridge, MA, USA.

[5]Analytic and Translational Genetics Unit, Department of Medicine, Massachusetts General Hospital, Boston, MA, USA.

[6]Department of Statistics and Data Science, Carnegie Mellon University, Pittsburgh, PA, USA.

[7]Pediatric Surgical Research Laboratories, Department of Surgery, Massachusetts General Hospital, Boston, MA, USA.

[8]Program in Bioinformatics and Integrative Genomics, Harvard Medical School, Boston, MA, USA.

[9]Department of Psychiatry, UCSF Weill Institute for Neurosciences, University of California San Francisco, San Francisco, CA, USA.

[10]Program in Neurogenetics, Department of Neurology, David Geffen School of Medicine, University of California Los Angeles, Los Angeles, CA, USA.

[11]Department of Psychiatry, University of Pittsburgh School of Medicine, Pittsburgh, PA, USA.

[12]Data Sciences Platform, The Broad Institute of MIT and Harvard, Cambridge, MA, USA.

[13]Seaver Autism Center for Research and Treatment, Icahn School of Medicine at Mount Sinai, New York, NY, USA.

[14]Department of Psychiatry, Icahn School of Medicine at Mount Sinai, New York, NY, USA.

[15]The Mindich Child Health and Development Institute, Icahn School of Medicine at Mount Sinai, New York, NY, USA.

[16]Genomics Platform, The Broad Institute of MIT and Harvard, Cambridge, MA, USA.

[17]Department of Medical Epidemiology and Biostatistics, Karolinska Institutet, Stockholm, Sweden.

[18]Department of Genetics and Genomic Sciences, Icahn School of Medicine at Mount Sinai, New York, NY, USA.

[19]Sorbonne Université, INSERM, CNRS, Neuroscience Paris Seine, Institut de Biologie Paris Seine, Paris, France.

[20]Department of Medical Sciences, University of Torino, Turin, Italy.

[21]Medical Genetics Unit, ‘Città della Salute e della Scienza’ University Hospital, Turin, Italy.

[22]Department of Pediatrics and Adolescent Medicine, Duchess of Kent Children’s Hospital, The University of Hong Kong, Hong Kong Special Administrative Region, China.

[23]Institute for Juvenile Research, Department of Psychiatry, University of Illinois at Chicago, Chicago, IL, USA.

[24]The John P Hussman Institute for Human Genomics, The University of Miami Miller School of Medicine, Miami, FL, USA.

[25]Department of Cellular, Computational and Integrative Biology, University of Trento, Trento, Italy.

[26]Department of Public Health and Pediatrics, University of Torino, Turin, Italy.

[27]Center for Autism Research and Translation, University of California Irvine, Irvine, CA, USA.

[28]The Research Institute at Nationwide Children's Hospital, Columbus, OH, USA.

[29]MIND (Medical Investigation of Neurodevelopmental Disorders) Institute, University of California Davis, Davis, CA, USA.

[30]Life and Health Sciences Research Institute, School of Medicine, University of Minho, Braga, Portugal.

[31]Department of Psychiatry, Massachusetts General Hospital and Harvard Medical School, Boston, MA, USA.

[32]Centro de Pesquisas sobre o Genoma Humano e Células tronco, Instituto de Biociências, Universidade de São Paulo, São Paulo, Brazil.

[33]Interdepartmental Program 'Autism 0-90', 'Gaetano Martino' University Hospital, University of Messina, Messina, Italy.

[34]Med Biotech Hub and Competence Center, Department of Medical Biotechnologies, University of Siena, Siena, Italy.

[35]Medical Genetics, University of Siena, Siena, Italy.

[36]Genetica Medica, Azienda Ospedaliera Universitaria Senese, Siena, Italy.

[37]Department of Molecular Physiology & Biophysics and Psychiatry, Vanderbilt University School of Medicine, Nashville, TN, USA.

[38]Vanderbilt Genetics Institute, Vanderbilt University School of Medicine, Nashville, TN, USA.

[39]Department of Biochemistry and Molecular Medicine, University of California Davis, School of Medicine, Sacramento, CA, USA.

[40]Department of Neurosciences, Biomedicine and Movement Sciences, Section of Biology and Genetics, University of Verona, Verona, Italy.

[41]Department of Diagnostic and Biomedical Sciences, University of Texas Health Science Center at Houston, School of Dentistry, Houston, TX, USA.

[42]Service for Neurodevelopmental Disorders, University Campus Bio-medico of Rome, Rome, Italy.

[43]Department of Molecular Biosciences, University of California Davis, School of Veterinary Medicine, Davis, CA, USA.

[44]Department of Human Genetics, Emory University School of Medicine, Atlanta, GA, USA.

[45]Friedman Brain Institute, Icahn School of Medicine at Mount Sinai, New York, NY, USA.

[46]Department of Neuroscience, Icahn School of Medicine at Mount Sinai, New York, NY, USA.

[47]Harvard Medical School, Boston, MA, USA.

[48]Institute for Molecular Medicine Finland (FIMM), University of Helsinki, Helsinki, Finland.

[49]Computational Biology Department, Carnegie Mellon University, Pittsburgh, PA, USA.

[82]These authors contributed equally: Jack M. Fu, F. Kyle Satterstrom, Minshi Peng, Harrison Brand.

Acknowledgements

We thank all of the individuals who participated in this research. We also thank all contributing investigators to the consortia datasets used here from the Autism Sequencing Consortium (ASC), the Simons Simplex Collection (SSC), Simons Powering Autism Research for Knowledge (SPARK) project, the iPSYCH project, the Deciphering Developmental Disorders (DDD) study and Schizophrenia Exome Meta-Analysis (SCHEMA). This work was supported by grants from the Simons Foundation for Autism Research Initiative (SSC-ASC Genomics Consortium 574598 to S.J.S., 575097 to B.D. and K.R., 573206 to M.E.T. and M.J.D., 571009 to J.D.); the SPARK project and SPARK analysis projects (606362 and 608540 to M.E.T., M.J.D., J.D.B., B.D., K.R. and S.J.S.); SFARI (736613 and 647371 to S.J.S.), NHGRI (HG008895 to M.J.D., S.G. and M.E.T.), NIMH (MH115957 and MH123155 to M.E.T., MH111658 and MH057881 to B.D., MH097849, MH111661 and MH100233 to J.D.B., MH109900 and MH123184 to K.R., MH111660 and MH129722 to M.J.D. and MH111662 and MH100027 to S.J.S.), NICHD (HD081256 and HD096326 to M.E.T.), AMED (JP21WM0425007 to N.O.) and the Beatrice and Samuel Seaver Foundation. J.M.F. was supported by an Autism Speaks Postdoctoral Fellowship and R.L.C. was supported by NSF GRFP 2017240332. E.D. was supported by Fondazione Italiana Autismo (FIA-2018/53).

References

1. Maenner MJ et al. Prevalence and characteristics of autism spectrum disorder among children aged 8 years—Autism and Developmental Disabilities Monitoring Network, 11 sites, United States, 2018. MMWR Surveill. Summ 70, 1–16 (2021).
2. Sandin S et al. The heritability of autism spectrum disorder. JAMA 318, 1182–1184 (2017). [PubMed: 28973605]
3. Grove J et al. Identification of common genetic risk variants for autism spectrum disorder. Nat. Genet 51, 431–444 (2019). [PubMed: 30804558]
4. Satterstrom FK et al. Large-scale exome sequencing study implicates both developmental and functional changes in the neurobiology of autism. Cell 180, 568–584.e23 (2020). [PubMed: 31981491]
5. Kaplanis J et al. Evidence for 28 genetic disorders discovered by combining healthcare and research data. Nature 586, 757–762 (2020). [PubMed: 33057194]
6. Coe BP et al. Neurodevelopmental disease genes implicated by de novo mutation and copy number variation morbidity. Nat. Genet 51, 106–116 (2019). [PubMed: 30559488]
7. Singh T et al. Rare coding variants in ten genes confer substantial risk for schizophrenia. Nature 604, 509–516 (2022). [PubMed: 35396579]
8. Wilfert AB, Turner TN, Murali SC et al. Recent ultra-rare inherited variants implicate new autism candidate risk genes. Nat. Genet 53, 1125–1134 10.1038/s41588-021-00899-8 (2021). [PubMed: 34312540]
9. Zhou X et al. Integrating de novo and inherited variants in over 42,607 autism cases identifies mutations in new moderate risk genes. Preprint at bioRxiv 10.1101/2021.10.08.21264256 (2021).

10. Lowther C et al. Systematic evaluation of genome sequencing as a first-tier diagnostic test for prenatal and pediatric disorders. Preprint at bioRxiv 10.1101/2020.08.12.248526 (2020).
11. Lord J et al. Prenatal exome sequencing analysis in fetal structural anomalies detected by ultrasonography (PAGE): a cohort study. Lancet 393, 747–757 (2019). [PubMed: 30712880]
12. Turner TN & Eichler EE The role of de novo noncoding regulatory mutations in neurodevelopmental disorders. Trends Neurosci. 42, 115–127 (2019). [PubMed: 30563709]
13. Moyses-Oliveira M, Yadav R, Erdin S & Talkowski ME New gene discoveries highlight functional convergence in autism and related neurodevelopmental disorders. Curr. Opin. Genet. Dev 65, 195–206 (2020). [PubMed: 32846283]
14. Sebat J et al. Strong association of de novo copy number mutations with autism. Science 316, 445–449 (2007). [PubMed: 17363630]
15. Talkowski ME et al. Sequencing chromosomal abnormalities reveals neurodevelopmental loci that confer risk across diagnostic boundaries. Cell 149, 525–537 (2012). [PubMed: 22521361]
16. Cooper GM et al. A copy number variation morbidity map of developmental delay. Nat. Genet 43, 838–846 (2011). [PubMed: 21841781]
17. Sanders SJ et al. Multiple recurrent de novo CNVs, including duplications of the 7q11.23 Williams syndrome region, are strongly associated with autism. Neuron 70, 863–885 (2011). [PubMed: 21658581]
18. Marshall CR et al. Structural variation of chromosomes in autism spectrum disorder. Am. J. Hum. Genet 82, 477–488 (2008). [PubMed: 18252227]
19. Pinto D et al. Convergence of genes and cellular pathways dysregulated in autism spectrum disorders. Am. J. Hum. Genet 94, 677–694 (2014). [PubMed: 24768552]
20. Iafrate AJ et al. Detection of large-scale variation in the human genome. Nat. Genet 36, 949–951 (2004). [PubMed: 15286789]
21. Lupski JR Genomic disorders ten years on. Genome Med. 1, 42 (2009). [PubMed: 19439022]
22. Collins RL et al. A cross-disorder dosage sensitivity map of the human genome. Preprint at medRxiv 10.1101/2021.01.26.21250098 (2021).
23. Byrska-Bishop M et al. High coverage whole genome sequencing of the expanded 1000 Genomes Project cohort including 602 trios. Preprint at bioRxiv 10.1101/2021.02.06.430068 (2021).
24. Mills RE et al. Mapping copy number variation by population-scale genome sequencing. Nature 470, 59–65 (2011). [PubMed: 21293372]
25. Collins RL et al. A structural variation reference for medical and population genetics. Nature 581, 444–451 (2020). [PubMed: 32461652]
26. Werling DM et al. An analytical framework for whole-genome sequence association studies and its implications for autism spectrum disorder. Nat. Genet 50, 727–736 (2018). [PubMed: 29700473]
27. Brandler WM et al. Paternally inherited cis-regulatory structural variants are associated with autism. Science 360, 327–331 (2018). [PubMed: 29674594]
28. Trost B et al. Genome-wide detection of tandem DNA repeats that are expanded in autism. Nature 586, 80–86 (2020). [PubMed: 32717741]
29. Turner TN et al. Genomic patterns of de novo mutation in simplex autism. Cell 171, 710–722.e12 (2017). [PubMed: 28965761]
30. Ruzzo EK et al. Inherited and de novo genetic risk for autism impacts shared networks. Cell 178, 850–866.e26 (2019). [PubMed: 31398340]
31. Chaisson MJP et al. Multi-platform discovery of haplotype-resolved structural variation in human genomes. Nat. Commun. 10, 1784 (2019). [PubMed: 30992455]
32. Ebert P et al. Haplotype-resolved diverse human genomes and integrated analysis of structural variation. Science 372, eabf7117 (2021). [PubMed: 33632895]
33. Zhao X et al. Expectations and blind spots for structural variation detection from long-read assemblies and short-read genome sequencing technologies. Am. J. Hum. Genet 108, 919–928 (2021). [PubMed: 33789087]
34. Karczewski KJ et al. The mutational constraint spectrum quantified from variation in 141,456 humans. Nature 581, 434–443 (2020). [PubMed: 32461654]

35. Samocha KE et al. Regional missense constraint improves variant deleteriousness prediction. Preprint at bioRxiv 10.1101/148353 (2017).
36. He X et al. Integrated model of de novo and inherited genetic variants yields greater power to identify risk genes. PLoS Genet. 9, e1003671 (2013). [PubMed: 23966865]
37. Sanders SJ et al. Insights into autism spectrum disorder genomic architecture and biology from 71 risk loci. Neuron 87, 1215–1233 (2015). [PubMed: 26402605]
38. O'Roak BJ et al. Sporadic autism exomes reveal a highly interconnected protein network of de novo mutations. Nature 485, 246–250 (2012). [PubMed: 22495309]
39. Glessner JT et al. Autism genome-wide copy number variation reveals ubiquitin and neuronal genes. Nature 459, 569–573 (2009). [PubMed: 19404257]
40. Pinto D et al. Comprehensive assessment of array-based platforms and calling algorithms for detection of copy number variants. Nat. Biotechnol 29, 512–520 (2011). [PubMed: 21552272]
41. Poplin R et al. Scaling accurate genetic variant discovery to tens of thousands of samples. Preprint at bioRxiv 10.1101/201178 (2017).
42. Belyeu JR et al. De novo structural mutation rates and gamete-of-origin biases revealed through genome sequencing of 2,396 families. Am. J. Hum. Genet 108, 597–607 (2021). [PubMed: 33675682]
43. Robinson EB, Lichtenstein P, Anckarsäter H, Happé F & Ronald A Examining and interpreting the female protective effect against autistic behavior. Proc. Natl. Acad. Sci. USA 110, 5258–5262 (2013). [PubMed: 23431162]
44. Szustakowski JD et al. Advancing human genetics research and drug discovery through exome sequencing of the UK Biobank. Nat. Genet 53, 942–948 (2021). [PubMed: 34183854]
45. Dong S et al. De novo insertions and deletions of predominantly paternal origin are associated with autism spectrum disorder. Cell Rep. 9, 16–23 (2014). [PubMed: 25284784]
46. Jónsson H et al. Parental influence on human germline de novo mutations in 1,548 trios from Iceland. Nature 549, 519–522 (2017). [PubMed: 28959963]
47. Duyzend MH et al. Maternal modifiers and parent-of-origin bias of the autism-associated 16p11.2 CNV. Am. J. Hum. Genet 98, 45–57 (2016). [PubMed: 26749307]
48. Simons Vip Consortium. Simons variation in individuals project (Simons VIP): a genetics-first approach to studying autism spectrum and related neurodevelopmental disorders. Neuron 73, 1063–1067 (2012). [PubMed: 22445335]
49. Doan RN et al. Recessive gene disruptions in autism spectrum disorder. Nat. Genet 51, 1092–1098 (2019). [PubMed: 31209396]
50. Russell G, Steer C & Golding J Social and demographic factors that influence the diagnosis of autistic spectrum disorders. Soc. Psychiatry Psychiatr. Epidemiol 46, 1283–1293 (2011). [PubMed: 20938640]
51. Doshi-Velez F, Ge Y & Kohane I Comorbidity clusters in autism spectrum disorders: an electronic health record time-series analysis. Pediatrics 133, e54–e63 (2014). [PubMed: 24323995]
52. Sanders SJ et al. A framework for the investigation of rare genetic disorders in neuropsychiatry. Nat. Med 25, 1477–1487 (2019). [PubMed: 31548702]
53. Nowakowski TJ et al. Spatiotemporal gene expression trajectories reveal developmental hierarchies of the human cortex. Science 358, 1318–1323 (2017). [PubMed: 29217575]
54. Carroll LS & Owen MJ Genetic overlap between autism, schizophrenia and bipolar disorder. Genome Med. 1, 102 (2009). [PubMed: 19886976]
55. Peng M, Li Y, Wamsley B, Wei Y & Roeder K Integration and transfer learning of single-cell transcriptomes via cFIT. Proc. Natl. Acad. Sci. USA 118, e2024383118 (2021). [PubMed: 33658382]
56. Peng M et al. Cell type hierarchy reconstruction via reconciliation of multi-resolution cluster tree. Nucleic Acids Res. 49, e91 (2021). [PubMed: 34125905]
57. Polioudakis D et al. A single-cell transcriptomic atlas of human neocortical development during mid-gestation. Neuron 103, 785–801.e8 (2019). [PubMed: 31303374]
58. van der Sluijs PJ et al. The ARID1B spectrum in 143 patients: from nonsyndromic intellectual disability to Coffin-Siris syndrome. Genet. Med 21, 1295–1307 (2019). [PubMed: 30349098]

59. Antaki D et al. A phenotypic spectrum of autism is attributable to the combined effects of rare variants, polygenic risk and sex. Nat. Genet 10.1038/s41588-022-01064-5 (2022).
60. Wang T et al. Integrated gene analyses of de novo mutations from 46,612 trios with autism and developmental disorders. Preprint at bioRxiv 10.1101/2021.09.15.460398 (2021).
61. Buxbaum JD et al. The autism sequencing consortium: large-scale, high-throughput sequencing in autism spectrum disorders. Neuron 76, 1052–1056 (2012). [PubMed: 23259942]
62. De Rubeis S et al. Synaptic, transcriptional and chromatin genes disrupted in autism. Nature 515, 209–215 (2014). [PubMed: 25363760]
63. Consortium SPARK. SPARK: a US cohort of 50,000 families to accelerate autism research. Neuron 97, 488–493 (2018). [PubMed: 29420931]
64. Van der Auwera GA & O'Connor BD Genomics in the Cloud: Using Docker, GATK, and WDL in Terra ('O'Reilly Media, Inc.', 2020).
65. Satterstrom FK et al. Autism spectrum disorder and attention deficit hyperactivity disorder have a similar burden of rare protein-truncating variants. Nat. Neurosci 22, 1961–1965 (2019). [PubMed: 31768057]
66. Tsirgiotis JM, Young RL & Weber N A mixed-methods investigation of diagnostician sex/gender-bias and challenges in assessing females for autism spectrum disorder. Preprint at J. Autism Dev. Disord 10.1007/s10803-021-05300-5 (2021).
67. Loomes R, Hull L & Mandy WPL What is the male-to-female ratio in autism spectrum disorder? A systematic review and meta-analysis. J. Am. Acad. Child Adolesc. Psychiatry 56, 466–474 (2017). [PubMed: 28545751]
68. Jiang H & Doerge RW Estimating the proportion of true null hypotheses for multiple comparisons. Cancer Inform. 6, 25–32 (2008). [PubMed: 19259400]
69. Ritchie ME et al. limma powers differential expression analyses for RNA-sequencing and microarray studies. Nucleic Acids Res. 43, e47 (2015). [PubMed: 25605792]
70. Benaglia T, Chauveau D, Hunter DR & Young D mixtools: an R package for analyzing finite mixture models. J. Stat. Softw 32, 1–29 (2009).

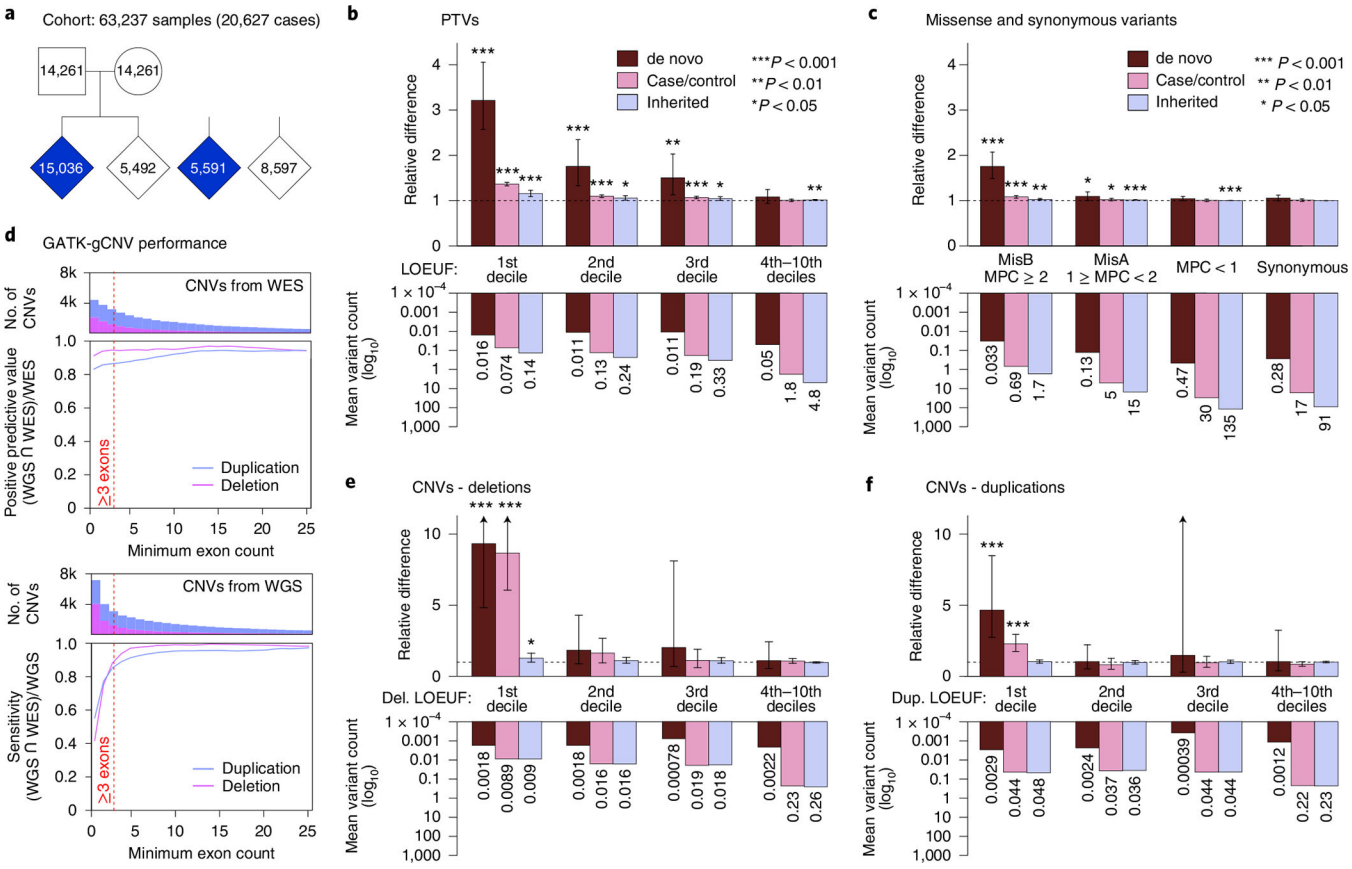

Fig. 1 |. Overview of SNV/indel and CNV rates in ASD by mode of inheritance and constraint.

a, The ASD cohort consisted of 49,049 family-based samples (15,036 cases) and 14,188 case-control samples (5,591 cases). One sample was a proband in one trio and a mother in another. **b**, The relative difference in PTV frequency between cases and unaffected controls (top) and average per sample variant count in unaffected controls (bottom) across inheritance classes (color) and LOEUF deciles (5,446 genes in top three deciles of LOEUF). Using a binomial test, cases were enriched for PTVs among the most constrained genes (lower LOEUF deciles), which weakened as negative selection against PTVs was relaxed (higher LOEUF deciles). **c**, Equivalent analyses were performed for missense variants annotated by MPC score and synonymous variants. Synonymous variants were not enriched in cases or controls, as evaluated via binomial tests. **d**, Benchmarking of the GATK-gCNV exome CNV discovery pipeline compared against WGS on overlapping samples achieved a sensitivity of 86% and PPV of 90% for rare CNVs (<1% site frequency) that spanned more than two captured exons (red line). **e**, The relative difference in variant frequency between cases and controls for deletions. Using binomial tests, we found that the enrichment of deletions (Del.) overlapping genes in the lowest LOEUF decile were stronger than PTVs in the same LOEUF deciles. **f**, Equivalent analysis for duplications (Dup.) demonstrated a similar pattern of enrichment compared with deletions but with more subtle relative differences. Statistical tests in **b**, **c**, **e** and **f** were two-sided binomial tests with 95% confidence interval error bars shown, *P* values (not corrected for multiple tests) and sample sizes are given in Supplementary Table 22.

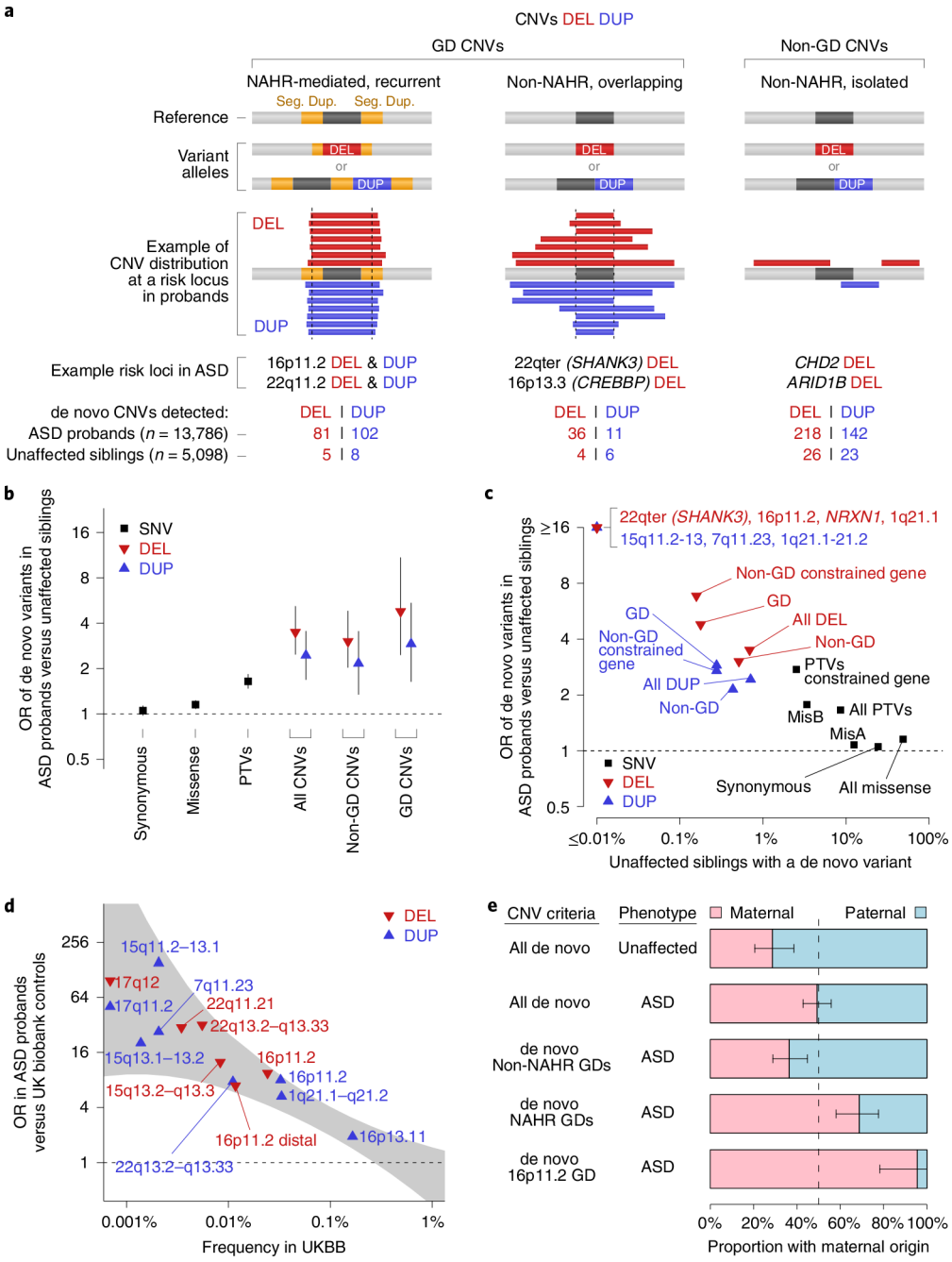

Fig. 2 |. Contribution of CNVs to ASD by mechanism and genomic location.

a, CNVs included deletions (DEL) or duplications (DUP) of genomic segments and involved a subset of recurrent sites known as GD loci. GDs mediated by NAHR harbored recurrent breakpoints localized to flanking segmental duplications (Seg. Dup.), whereas non-NAHR GDs did not. **b**, De novo CNVs were highly enriched in affected cases compared with unaffected offspring (Fisher's exact test) and the effect size was greater than that observed in de novo PTVs or de novo missense variants (logistic regression). **c**, ORs for de novo GD CNVs in probands compared with unaffected siblings, a subset of which have no observed de novo CNVs in unaffected individuals in this cohort (for example, 16p11.2 deletions,

15q11.2-q13 duplications). **d**, Analysis of all GDs (de novo and inherited) in ASD cases compared with GDs in a population-based cohort (UKBB) discovered using GATK-gCNV with identical parameters, with LOESS-smoothed bands of the 95% confidence interval of the OR in gray. **e**, Parent-of-origin analysis of de novo CNVs using binomial tests showed maternal bias for NAHR-mediated CNVs at GD regions, which was most pronounced for the 16p11.2 GD as previously described[47]. Statistical tests in **b** and **c** were Fisher's exact test with 95% confidence interval plotted as error bars, *P* values (not corrected for multiple tests) and sample sizes are located in Supplementary Table 22; statistical tests in **d** were Fisher's exact test of carrier status in 13,786 unique ASD cases and 143,532 unique UK biobank controls, *P* values (not corrected for multiple tests) are located in Supplementary Table 10; statistical tests in **e** were binomial test with 95% confidence interval plotted as error bars, sample sizes and *P* values (not corrected for multiple tests) are located in Supplementary Table 22.

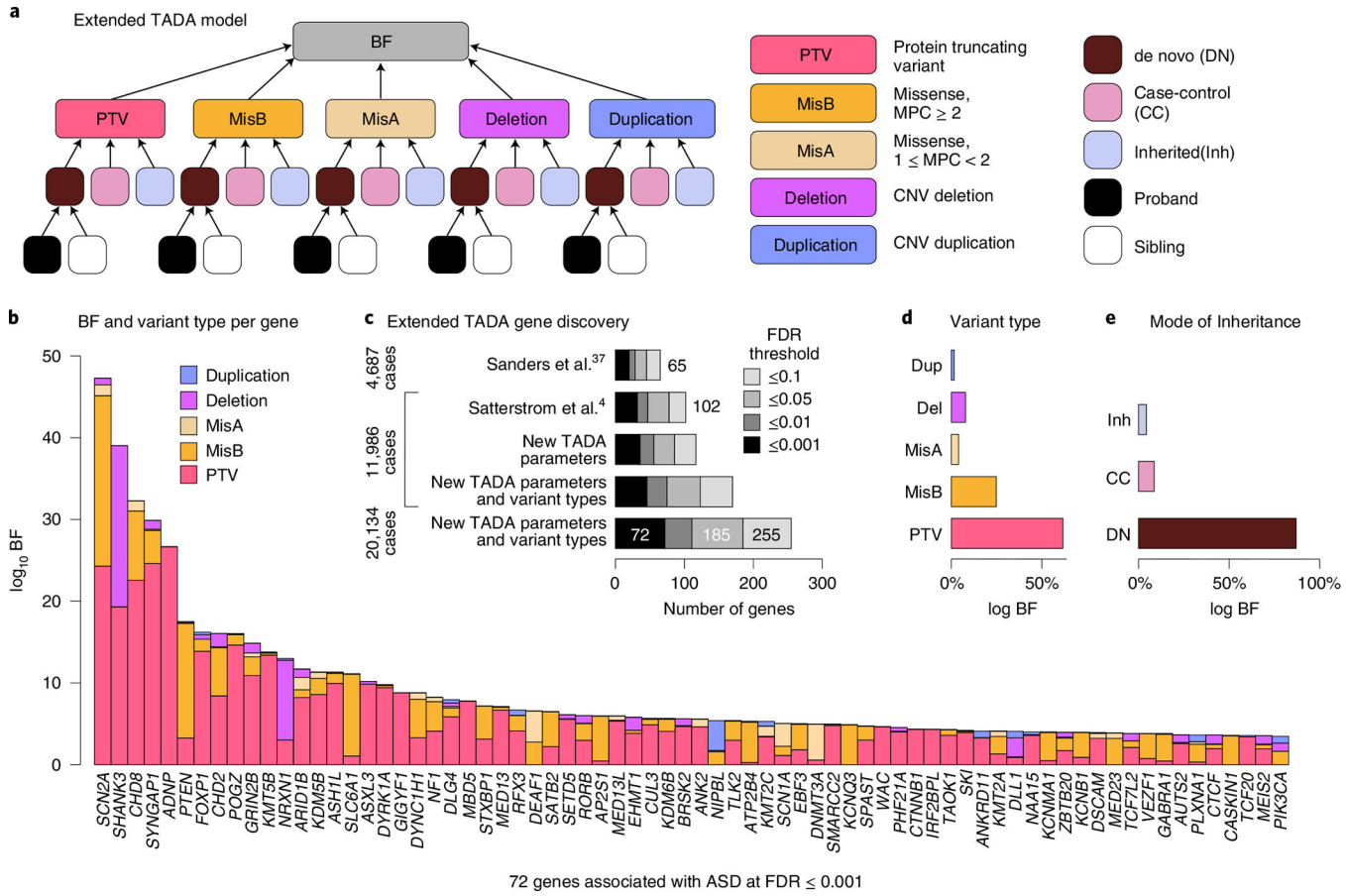

Fig. 3 |. Integrating variant types and inheritance classes improves association power and reveals mutational biases within candidate genes.

a, Our new implementation of the TADA model included de novo, case-control and rare inherited modules for each variant type: PTV, MisB, MisA, deletion and duplication. We leveraged information from ASD probands as well as unaffected siblings in evaluating the effect of de novo variants. **b**, The evidence of ASD association contributed by each variant type for each of the 72 ASD genes with FDR ≤ 0.001. Some genes were associated predominantly with missense variants and duplications (for example, *PTEN* and *SLC6A1*), suggesting mechanisms other than haploinsufficiency. **c**, Applying TADA to our aggregated ASD dataset yielded 72 genes at FDR ≤ 0.001, compared with 32 and 19 genes at the same threshold in previous studies on a subset of the samples[4,37]. Our expanded TADA model improved the integration of available evidence of association and increased gene discovery at equivalent statistical thresholds on the same datasets. **d**, We quantified the relative contribution of variant class and mode of inheritance to these 72 ASD-associated genes, demonstrating that de novo PTVs and MisB variants represented the strongest contributions to the association signals. **e**, Association evidence (BF) was predominantly driven by de novo variants. The statistical test used in **b** was the extended TADA model.

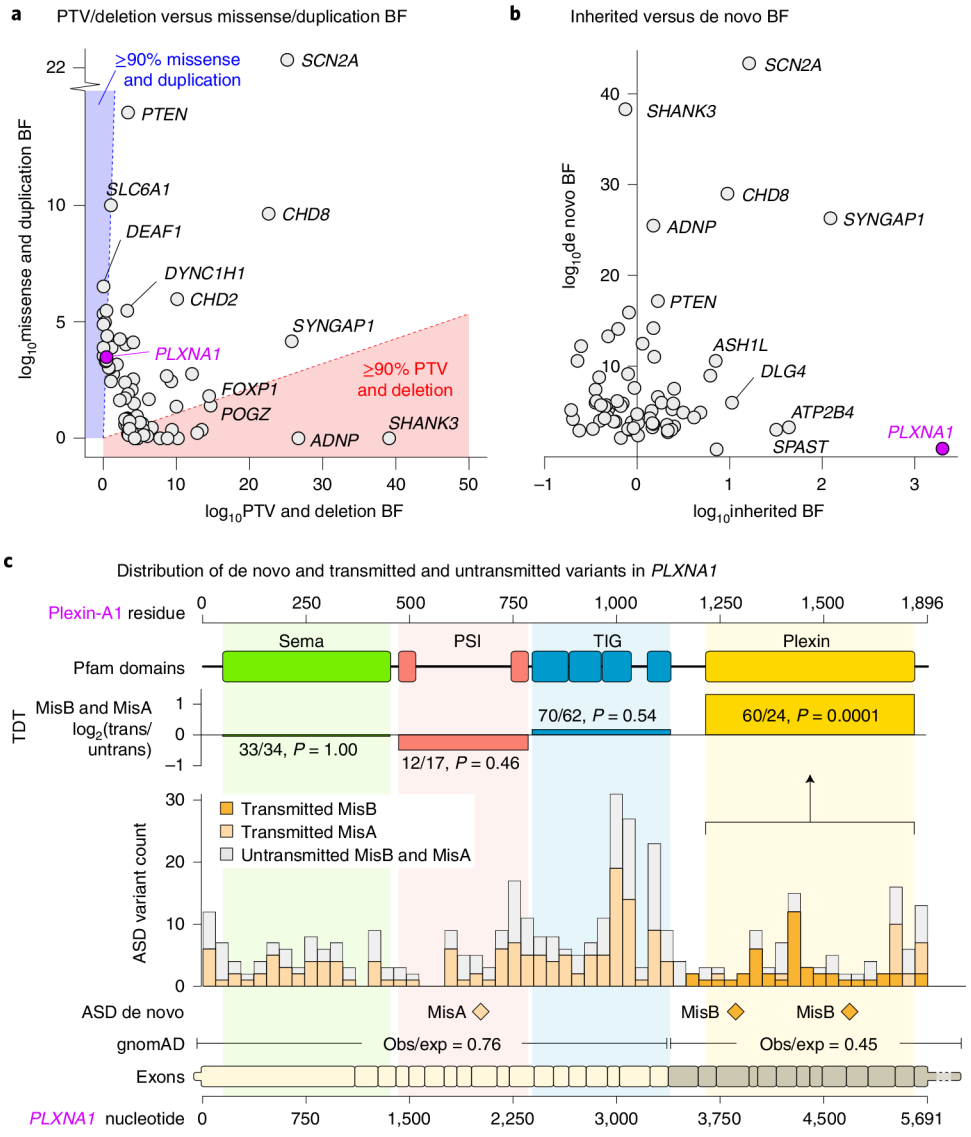

Fig. 4 |. Relative contribution of evidence types in ASD risk genes.

a, The relative evidence of ASD association in the extended TADA model ($\log_{10}$BF) for the 72 ASD risk genes (FDR ≤ 0.001) shown for likely loss-of-function mechanism (PTVs and deletions) on the *x* axis versus variants that may act via alternative mechanisms (missense variants and duplications) on the *y* axis. **b**, Plot of the relative association evidence from de novo (*y* axis) versus inherited (*x* axis) variation for the 72 ASD risk genes. **c**, Evidence for ASD association for the gene *PLXNA1* was derived from de novo and inherited missense variants localized to the Plexin domain at the C-terminus of the Plexin-A1 protein. Statistical test in **c** was the transmission disequilibrium test. Obs/exp, observed/expected.

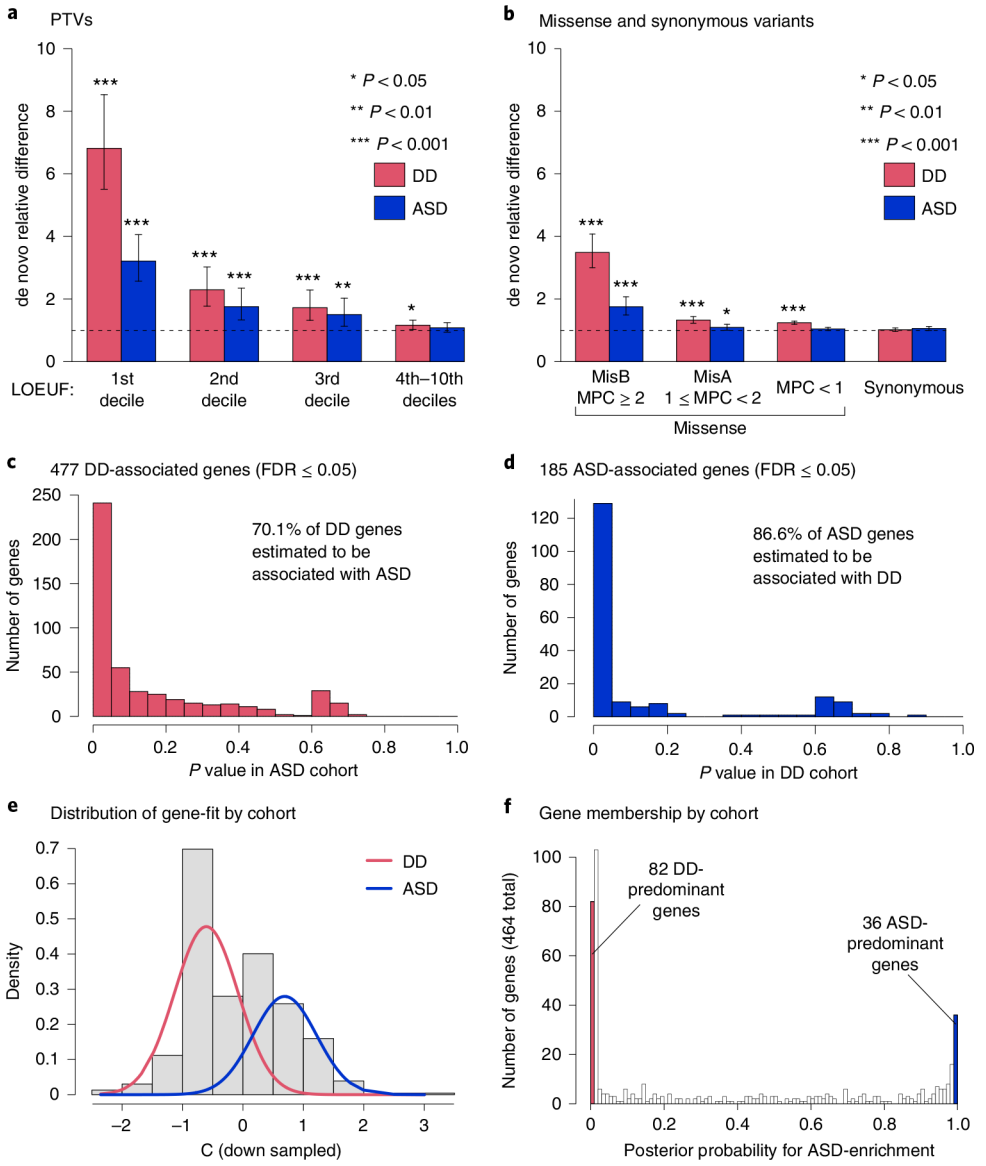

Fig. 5 |. Integration of ASD and DD datasets.

We performed meta-analysis of the ASD cohort with the 31,058 DD trios reported in Kaplanis et al.[5] (n = 46,094 combined NDD cases). **a**, Relative difference of de novo PTVs in ASD and DD cohorts across deciles of constraint as measured by LOEUF. **b**, Relative difference of de novo missense variants in DD and ASD cohorts across categories of MPC scores. **c**, To explore overlap in association evidence across ASD and DD risk genes, we considered the 477 TADA-DD genes with FDR ≤ 0.05. We evaluated their P value distributions converted from TADA-ASD FDRs and observed nonuniformity suggesting that, in aggregate, 70.1% of these genes also had evidence of association with ASD. **d**, In the complementary analysis of the 185 TADA-ASD genes with FDR ≤ 0.05, we looked at their P value distributions converted from TADA-DD FDRs and again observed high nonuniformity, suggesting that, in aggregate, 86.6% of these genes had evidence of association with DD. **e**, Using PTV and MisB variant data, we devised a chi-squared

statistic, denoted the C statistic, to measure if a gene has more observed variants in one cohort relative to the other. A mixture model was used to deconvolve the commingled distributions. **f**, We transformed the fitted mixture distribution into posterior probability for ASD enrichment. Using a cutoff of <0.01, we found 82 DD-predominant genes, while using a cutoff of >0.99 we found 36 ASD-predominant genes. Statistical tests: **a**,**b**, two-sided binomial test, with 95% confidence interval error bars shown; *P* values (not corrected for multiple tests) and sample sizes located in Supplementary Table 22; **c**,**d**, R v.3.5.3 package limma_3.38.3; **e**,**f**, mixture model.

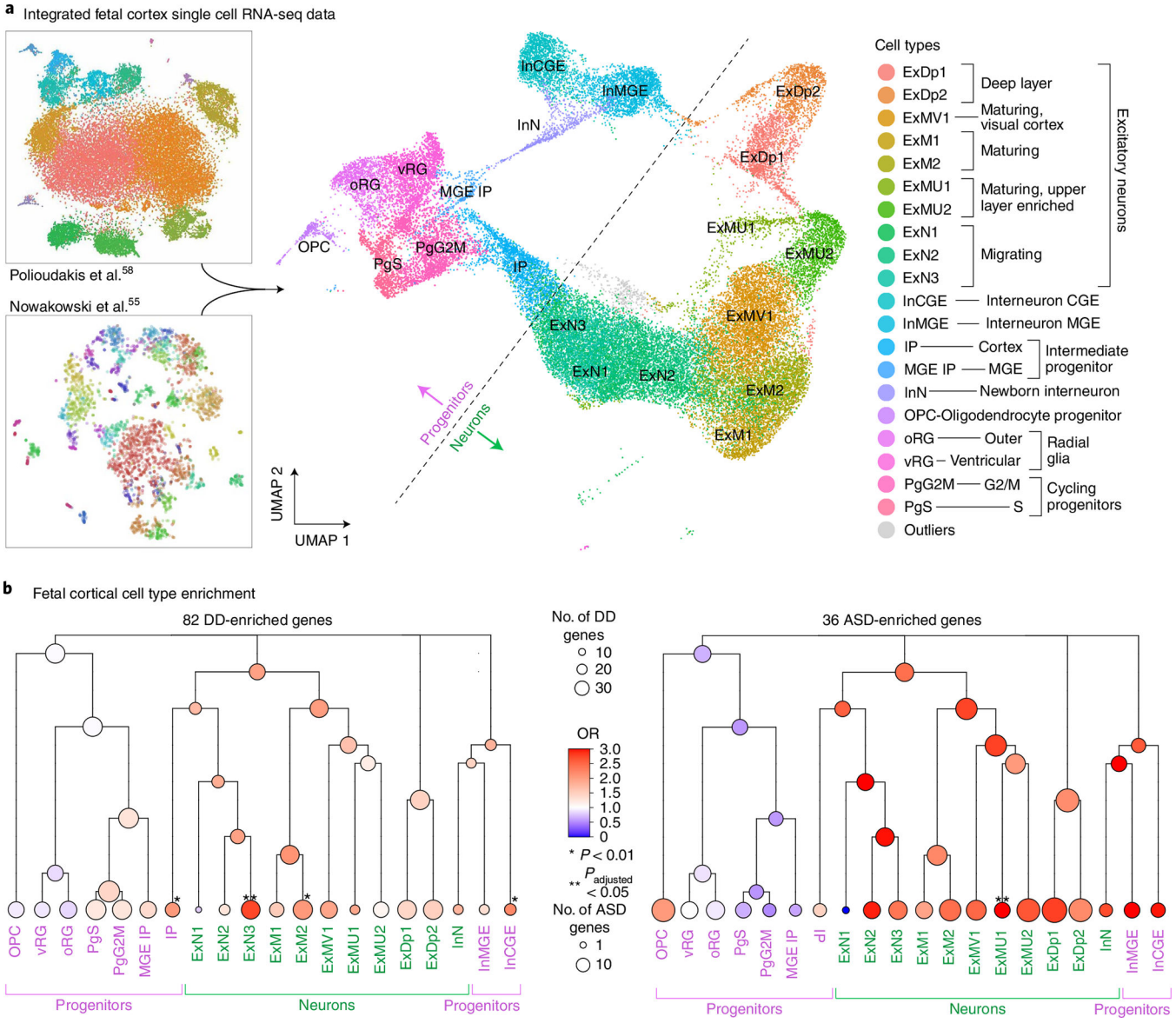

Fig. 6 |. Single-cell data reveals differential neuronal layers impacted by ASD and DD genes.

a, A UMAP plot visualization after integrating two studies[53,54] that provided single-cell gene expression of human fetal brains consisting of 37,000 cortical cells at 6–27 weeks postconception. Similar cell types from the two batches were grouped together while preserving cells unique to either study. See Supplementary Table 17 for unabbreviated cell type labels and classifications to ‘progenitor’ and ‘neuron’ types. **b**, Both ASD- and DD-predominant genes (right and left, respectively) were found to be enriched in interneurons and excitatory neurons compared to glial cells. Compared with DD-predominant genes, ASD-predominant genes were relatively more neuron-enriched than progenitor-enriched. The developmental trajectory of excitatory neurons was approximately recapitulated in the UMAP, starting with OPC and other progenitor cells and ending with maturing upper-layer

enriched and deep layer excitatory neurons. For interneurons, InCGE and InMGE were precursors to InN. Statistical test used in **b** was Fisher's exact test.